1975

Stresses in several types of bridges, May 1975, M.S. thesis

Andrew C. Coates

STRESSES IN SEVERAL TYPES OF BRIDGES

by

Andrew C. Coates

STRESSES IN SEVERAL TYPES OF BRIDGES

by

Andrew C. Coates

A Thesis
Presented to the Graduate Committee
of Lehigh University
in Candidacy for the Degree of
Master of Science
in
Civil Engineering

May 1975

This thesis is accepted and approved in partial fulfillment of the requirements for the degree of Master of Science in Civil Engineering.

May 9, 1975

Dr. Ben T. Yen

Dr. David A. VanHorn
Chairman

ACKNOWLEDGMENTS

This thesis presents the results of field tests of four Pennsylvania Bridges. These field tests were undertaken as part of PennDOT Research Project 72-3, High Cycle Fatigue of Welded Bridge Details, sponsored by the Pennsylvania Department of Transportation and the Federal Highway Administration. The project is being conducted at Fritz Engineering Laboratory, Department of Civil Engineering, Lehigh University. Dr. Lynn S. Beedle is Director of the Laboratory and Dr. David A. VanHorn is the Chairman of the Department.

Thanks are due Mr. Hugh T. Sutherland for his assistance in the acquisition of test data. A number of Fritz Engineering Laboratory staff under the supervision of Mr. K. R. Harpel assisted with the field work. Mr. Richard N. Sopko provided the photographs and Donald P. Erb assisted with the drawings. The sleepless nights of Dr. Ben T. Yen are gratefully acknowledged as well as the guidance of Drs. John W. Fisher and J. Hartley Daniels. Special thanks are due to Mrs. Dorothy Fielding for typing the manuscript.

TABLE OF CONTENTS

TABLE OF CONTENTS (continued)

LIST OF TABLES

LIST OF FIGURES

LIST OF FIGURES (continued)

LIST OF FIGURES (continued)

ABSTRACT

Strain measurements were taken at several structural details on four bridges in Pennsylvania. Strain gages were mounted on tie-plates, coverplated beams and diaphragm connections to beams, floor beam details, girders and girder details and diaphragms. An automatic data acquisition system, amplifier and magnetic tape units, and an ultra violet analog trace recorder were used to record the data. The tieplates were subjected to horizontal in-plane bending stresses. Earlier inspections revealed numerous tieplate rivet failures at one bridge.

The stresses at details were compared with the 1974 AASHTO Specifications to evaluate the fatigue strength of the details. All details were found to have sufficient fatigue strength. Only the tie-plates on one bridge might experience fatigue failure in the future if current loading and geometrical conditions continue. A model was presented to explain the horizontal bending stresses in the tieplates and the rivet failures. Both phenomenon were due to a horizontal displacement of the tieplate relative to the stringers. The displacement was caused by the elongation and shortening of the top flange of the girders under live load. The measured stress spectrum in several tieplates on a bridge and the estimated truck traffic during the structure's life were used to estimate the cumulative fatigue damage in those tieplates. Good correlation was obtained with constant cycle laboratory fatigue test results using the root-mean-square stress range and Miner's hypothesis.

1. INTRODUCTION AND DESCRIPTION OF BRIDGES

1.1 Introduction

Several steel bridges in North America have experienced fatigue cracks in the past few years. Details such as the ends of coverplates, web and flange attachments, and tieplates connecting transverse floor beams and outrigger brackets to main girders have exhibited fatigue cracks at weld toe terminations, tack welds or rivet holes. Recently rivet failures have also been discovered in the tie-plate details. South Bridge on Interstate Route 83 in Pennsylvania, the Allegheny River Bridge on the Pennsylvania Turnpike (1), the Lehigh River and Canal Bridges on U. S. Route 22 in Pennsylvania (2), the Yellow Mill Pond Bridge on the Connecticut Turnpike (3) and the Aquasabon River Bridge in Ontario, Canada (4) are among the bridges where cracks or rivet failures have been encountered.

Field tests have been carried out at the Lehigh Canal (2) and Allegheny River Bridges (1) in an attempt to correlate the traffic crossing the bridge with the stresses recorded in the details studied and the occurrence of fatigue cracking. The field data in turn were compared to results of constant cycle fatigue tests conducted in laboratories.

Laboratory studies indicate that stress range (live load and impact stress) controls the fatigue behavior of structural details (5) and (6). The crack growth threshold is not well defined for most details.

This report presents the results of the field testing of four Pennsylvania bridges. Stresses at various details were recorded. As in the Lehigh Canal and Allegheny River Bridge studies, correlations are made between the traffic over the bridges, the recorded stresses and laboratory test results. The field data were analyzed to determine the reasons for fatigue cracking in tieplates and the rivet failures. Recommendations to control these failures are made on the basis of analysis of the data.

1.2 Description of Bridges

The four bridges which were tested are the Columbia-Wrightsville Bridge (58926) of Pa. Route 462 over the Susquehanna River at Columbia, Pennsylvania, the Interstate Route 81 Susquehanna River Bridge (S8787) (also called the North Bridge) and the South Bridge (on John Ham's Bridge) (S2378) which carries Interstate Route 83 over the same river in Harrisburg, and a bridge on U. S. Route 202 over the Green Hill Road (S8333) near West Chester, Pennsylvania. For convenience, the last of the above four is called the West-Chester Bridge in this report.

The Columbia-Wrightsville Bridge, Fig. 1, consists of twin bridges which carry the east and west bound lanes of Pa. 462 over the

Susquehanna River. Each of the twin bridges is composed of a 44 span, continuous welded plate girder bridge and two simply supported composite I-beam approach spans. The east approach span and the adjacent first continuous span were chosen for testing due to their accessibility.

The plan (minus the concrete deck) and elevation of the 62'-4" approach span and the 95'-3" first span are shown in Fig. 2 along with the approximate locations of the strain gages. The exact location of the gages is given later.

The load carrying system of the approach span consists of six longitudinal, W33 x 118, beams complete with an 8" reinforced concrete deck. The beams are 2' 8-7/8" deep with a 24' long cover-plate on the bottom flange.

A typical cross section of the first continuous span is shown in Fig. 3a. The girders are 9'-2" deep. The load carrying system of this span consists of seven floor beams (five, W27 x 88 and two, welded plate sections), outrigger brackets, two exterior stringers (C18 x 51.9), two interior stringers (W18 x 45), and an 8-1/2" reinforced concrete deck. The tieplate detail is sketched in Fig. 3b. The tieplates are embedded in concrete.

The Columbia-Wrightsville Bridge was gaged at the following details: the ends of coverplates in the approach span, tieplates, the connections of the catwalk to the floor beams, the knee brackets connecting the girder and the floor beam, a gusset plate welded to a girder flange, and the girder flange at a flange splice.

The Interstate Route 81 Susquehanna River Bridge is a twin bridge each of which consists of a 34 span continuous girder bridge and ten approach spans.

The second span of the continuous girder on the west end of the eastbound bridge was instrumented because of its nearness to a power source and its accessibility. The tested span had two traffic lanes and the acceleration lane for an on-ramp.

The plan (with the concrete deck removed) and elevation views of the 136' test span are shown in Fig. 4 together with the approximate strain gage locations. The depth of the longitudinal girders is 10' 2-1/4". A cross section of the instrumented span is given in Fig. 5a. A three girder system is used in this span due to the acceleration lane of the on-ramp. There are 18 floor beams with outrigger brackets, 27 stringers and an 8-1/2" reinforced concrete deck in the test span. As in the Columbia-Wrightsville Bridge the outrigger brackets and the floor beams are connected to the girders by tieplates which are embedded in the concrete deck. The Interstate Route 81 Susquehanna River Bridge tieplate detail is found in Fig. 5b. At the time of test (November 1974) there was little truck traffic over the bridge.

Since the structural arrangment of the Interstate Route 81 Susquehanna River Bridge is quite similar to that of the Columbian-Wrightsville Bridge, structural details in the former corresponding to those of the latter were instrumented for comparison purposes.

These details were: catwalk connections to the floor beams, tieplates, knee brackets and gusset plates welded to the girder flange.

The South Bridge in Harrisburg, see Fig. 6, consists of a 20-span continuous girder bridge and six approach spans. ~~East~~ NORTH and ~~westbound~~ SOUTHBOUND lanes are on the same superstructure. The east end span was investigated because of its accessibility.

Figure 7 depicts the plan (minus the concrete deck) and elevation of the 184' 6-3/4" end span. The depth of the longitudinal girders varies from 8'-1/2" at pier 21 to 11' 11-13/16" at the interior piers. A typical cross section is shown in Fig. 8a. The test span's steel skeleton is made up of 6 built-up floor beams (web: 68" x 3/8", flanges: 2 angles 6" x 6" x 1/2"), the same number of outrigger brackets and 16 stringers (W21 x 68). The roadway is a 7-1/2" reinforced concrete deck. Tieplates connecting the outrigger brackets and the floor beams to the main girder are not embedded in the concrete deck. A typical tieplate detail is shown in Fig. 8b.

The arrangement of girders, floor beams and stringers of the South Bridge is essentially the same as that of the Lehigh Canal and Allegheny River Bridges. The stringers rest on the top flanges of the floor beams which are at approximately the same level as the top flange of the girders. In both the Lehigh Canal and the Allegheny River bridges the tieplates experienced fatigue cracks. For this reason most of the gages on the South Bridge were placed on the tieplates. A girder and a stringer were also instrumented.

At the time of the tests (August and November 1973) no fatigue cracks were observed in South Bridge's tieplates. Numerous rivet failures, though, have been discovered in the tieplate detail (7). These failures occur primarily in the rivets connecting the first inboard stringer and the tieplate to the floor beams, or in some cases in those rivets connecting the girder to the tieplate. The rivets that failed at the stringer connection cracked through the shank. No information was available on the mode of failure that occurred in the rivets connecting the tieplate and the girder. South Bridge is subjected to very heavy truck traffic at all hours of the day and night. It was opened to traffic in October of 1960.

The West Chester Bridges, Figs. 9 and 10, carry the north and southbound lanes of U. S. Route 202 over Green Hill Road near West Chester, Pennsylvania. These short, skewed, coverplated beam bridges consist of seven simply supported beams (W27 x 84) composite with an 8" reinforced concrete deck and braced by diaphragms (C15 x 33.9). These failures occur primarily in the rivets connecting the first inbound stringer and the tieplate to the floor beam, or in some cases in those rivets connecting the girder to the tieplate. The west view and cross section of one of the bridges are shown in Fig. 11. A plan view of both bridges (without the concrete deck) is sketched in Fig. 12. Gages were placed on the beams near midspan and at the ends of the coverplates, on the diaphragms, and at the diaphrgam connection.

2. STRAIN MONITORING AND TESTING PROCEDURE

2.1 Strain Gages

To obtain live load stresses at the details which have experienced fatigue failure in the laboratory or in the field, electrical resistance strain gages were mounted at these details. The approximate locations of all gages are shown on the plan views of the respective bridges. Appendix A together with Figs. 13 to 19 give the exact locations.

A plan view of typical gage locations on a tieplate is shown in Fig. 13a. Tieplates are used to connect floor beams and outrigger brackets to the longitudinal girders. At Columbia-Wrightsville Bridge, the gages were mounted on the bottom of the tieplate between the top flange of the girder and that of the floor beam or outrigger bracket. The tieplates of the Interstate Route 81 Susquehanna River Bridge. Most of the tieplate gages on the South Bridge were on the top surface of the plate, with a few under the tie plate at pier 21.

The bottom view of coverplate details are sketched in Fig. 13b. This detail occurred at the West Chester and Columbia-Wrightsville Bridges. The coverplate was wider than the beam on the Columbia-Wrightsville Bridge. At West Chester the coverplate was narrower than the beam.

The plan and elevation of the knee bracket connection of the Columbia-Wrightsville and the Interstate Route 81 Susquehanna Bridge is depicted in Fig. 14 indicating the gage locations. The knee brackets connect the girder and the floor beam and is also connected to the tie plate. Design live load stresses are fairly high at these brackets.

The connections of the catwalks to the bottom of the floor beams at the Columbia-Wrightsville and the Interstate Route 81 Susquehanna River Bridges create a stress raising detail at the tension flanges of the floor beams. Gage locations for this detail are given in the elevation and plan views of the detail in Fig. 15.

At South Bridge one gage was mounted on a stringer and four gages on a girder. Their locations are shown in Figs. 16a and 16b, respectively. Gages 52 and 53, Fig. 7, were located on the top face of the top flange of the girder and gages 35 and 36 on the bottom face of the bottom flange.

Diaphragms and diaphragm connections to longitudinal bridge beams were instrumented at the West Chester Bridge. Gages on the skewed beam diaphragms were mounted on the bottom flange, Fig. 17. The locations of gages on the longitudinal beams at the diaphragm connection are indicated in the elevation and plan views of the longitudinal beams in Fig. 18. Two gages, 23 and 28, Fig. 12, were mounted on the flange of the beam directly below the connection.

A flange splice in the eastbound test span was instrumented to monitor the live load stresses at a girder splice. One strain

gage was installed on the flange plate at the splice, Fig. 2 and 19a.

All strain gages were 1/4" electrical resistance foil gages. Weatherproof coatings were added after mounting to protect the gages from moisture and the environment. To minimize the effects of temperature changes, the gages were connected to temperature compensation gages and plates.

2.2 Recording Systems

Live load strain variations were recorded using one or two of three systems. An automatic data acquisition system, a magnetic tape recorder, and an analog trace recorder. At the West Chester and Columbia-Wrightsville Bridges the Federal Highway Administration's automatic data acquisition system was used. This system, located in a van consists of an amplifier, an analog-to-digital signal converter, a computer and a teletype machine. The operation of this system has been described in previous reports (1, 2). The output from this system is frequencies of stress range occurrences at the gage points. South Bridge strain signals were fed into the Federal Highway Administration system's amplifiers and recorded on magnetic tapes using a recorder of the Pennsylvania Department of Transportation. Ultra violet analog trace recordings were made at all four bridges. These traces recorded the live load variation of strain with time. The analog recorder also utilized the amplifiers of the Federal Highway Administration's system. This enabled the strain variations of several gages to be monitored by two systems simultaneously.

2.3 Loading

Strains were measured under two types of loading: a known load (test truck) and random loads (normal traffic). A Federal Highway Administration test truck was used at each bridge except the West Chester Bridge. Its use permitted the magnitudes of live load strains to be determined for a known load. Measurements of live load strain variation due to normal traffic were taken at each bridge except the Interstate Route 81 Susquehanna River Bridge which had little truck traffic at the time of the test. These measurements provided data for histograms or frequency distributions of stress ranges which were correlated with constant cycle laboratory test results for the evaluation of fatigue strengths of the bridge detail.

Truck traffic crossing the bridge was counted for periods of time and was classified usually according to the Federal Highway Administration designation, Fig. 20. These observations were sometimes taken in conjunction with the ultra violet analog traces so that stresses and the type of truck could be correlated.

3. MEASURED STRESSES IN BRIDGE DETAILS

3.1 Maximum Stress

The main purpose of the field tests was to determine the stresses caused by truck traffic at the bridge details so as to evaluate the performance of the bridge with respect to fatigue. The recorded stresses were live load plus impact stresses fluctuating with respect to the dead load stresses. A typical analog trace of stress versus time is shown in Fig. 21. It is not necessary for the evaluation of the fatigue strength of a structural detail to know its dead load stress since laboratory test results indicate that stress range is the controlling parameter of fatigue strength (5, 6). Stress range is defined as the difference between a maximum stress and the following minimum stress, Fig. 21.

Stress values were obtained by converting recorded strain values assuming a modulus of elasticity of steel of thirty million pounds per square inch. The maximum live load stresses recorded by the analog traces are summarized in Tables 1 to 3 along with the live load plus impact design stresses where they were available. The maximum live load stresses for a gage is defined as the absolute value of the greatest live load stress due to live load plus impact recorded by the analog traces during the testing period. Tables 1 to 3 also list the maximum stress ranges recorded either by the Federal

Highway Administration automatic data acquisition system or the analog traces. Locations subjected to high maximum live load stresses also experienced high stress ranges.

3.2 Stresses in Details

The following sections (3.1.2 to 3.1.7) present the maximum live load stresses, the maximum stress ranges and observations about this variation of stress with time for the bridge details under study. The maximum stresses are compared with the design stresses to see how closely the design values were to the actual stresses. The maximum stress ranges are used in Sect. 3.2 as the variable for determining whether or not a particular detail is likely to experience fatigue cracking. Using the analog traces, the variations of stress with time can be compared for similar details at more than one bridge.

3.2.1 Tieplates

Two types of tieplate detail were encountered in the bridges studied: open and embedded. The stringers and the girders at South Bridge, Fig. 8a, are not on the same level and thus the tieplates are exposed (open) and are not composite with the deck. The Columbia-Wrightsville and Interstate Route 81 Susquehanna River Bridges, Figs. 3a and 5a, have the concrete deck resting on both the stringers and the girders. The tieplates are embedded in the concrete deck. The open tieplates recorded maximum live load stresses and stress ranges in the order of ten times higher than those experienced by the embedded ones.

The variation of stress with time for a typical tieplate from each of the three tie-plated bridges is traced in Fig. 22. In each instance, the loading was the Federal Highway Administration test truck simulating a HS 20-44 loading. The speeds of the truck during these tests were also comparable (45-55 mph).

Gage 50 at South Bridge is located on a tieplate at pier 20, see Figs. 7 and 13 and Table 3. The stress excursion takes place in approximately 6 sec. The test truck traveling in the south bound lane at approximately 45 mph traverses about two and a half spans (400') in this interval. Stress reversal occurs as the truck moves from one span to the next. The jagged appearance of the analog trace is caused by small vibrational stresses. By the time the truck reaches the third span it has little effect on the tieplate in the first span. The end of the stress excursion consists of the damping out of the vibrational stresses.

The tieplate, gage 11, for the Columbia-Wrightsville Bridge in Fig. 22 is located at pier 44, Fig. 2. Here the stress excursion occurs in about 3.5 sec. This interval corresponds to the time it takes the test truck to cross two spans (250') at a speed of 50 mph. Again the presence of the truck is not felt when it is more than one span away. Qualitatively the tieplates at the Columbia-Wrightsville and South Bridges have the same response in that stress reversal occurs as the truck moves from one span to the next. However, the trace for the tieplate of the Columbia-Wrightsville Bridge is smoother than the one for the tieplate of the South Bridge, indicating that there was less vibration at the former than the latter bridge. Also,

the magnitude of the maximum live load stress and the stress range are both lower in the Columbia-Wrightsville Bridge. The stress ranges for the traces shown are 9.0 ksi at South Bridge and 1.5 ksi at Columbia-Wrightsville Bridge. The reason for those differences in vibrational behavior and stresses is attributed to the fact that the embedment of the top flange of the girder and the tieplate in concrete significantly increases the monolithic nature of the deck girder load carrying system. This decreases the vibrations of the bridge and reduces the cause of high stresses in the tieplates. The evaluation of tieplate stresses is presented in Chapter 4.

The stress time trace of a tieplate in the Interstate Route 81 Susquehanna River Bridge, gage 13 of Fig. 22, is qualitatively different from the preceding two and has a very small stress range (0.4 ksi). The stress excursion takes place in about one second. The test truck in this time period covers about half a span (70') with a speed of 50 mph. This is about twice the length of the test truck. This and the fact that the excursion consists of two basically identical humps implies strongly that at this tieplate the stress is axle dependent rather than vehicle dependent. As in the Columbia-Wrightsville Bridge the tieplates are embedded in concrete and there are no appreciable vibrational stresses.

During the period of testing, the highest recorded live load stress for the South Bridge open tieplates was 11.0 ksi. The maximum stress range was 14.0 ksi. These values are comparable to those recorded in the Lehigh Canal Bridge and the Allegheny River Bridge Bridge (1, 2). The live load stress distribution in the tieplate at

a given instant of time is shown in Fig. 23. It indicates that the tieplate was subjected to high bending stresses in the horizontal plane with relatively small axial elongation or vertical bending under live load. This type of stress distribution was typical for all the South Bridge tieplates. Figure 24 gives a schematic plan view of South Bridge tieplates. The numbers at the tieplates are the maximum live load stresses recorded by the gages near the edges of the tieplates where the horizontal bending stresses are the highest. Generally, the higher stresses were at or near pier 21, which is the beginning of the continuous span bridge, Fig. 7. Stress magnitudes were smaller towards the live load point of contraflexure near mid-span. A further examination of tieplate stresses is made in Chapter 4.

The embedded tieplates at the Columbia-Wrightsville Bridge had a maximum recorded live load stress of 1.0 ksi and a maximum stress range of 1.5 ksi. A typical live load stress distribution for a tieplate on this bridge at a given time, depicted in Fig. 25, shows that the tieplate was subjected to horizontal bending. The magnitudes of these stresses were much lower than those in the South Bridge.

The tieplates of Interstate Route 81 Susquehanna River Bridge also embedded in concrete. A maximum live load stress of 0.5 ksi and a maximum stress range of 0.5 ksi were recorded. There were only three functioning gages on the tieplates at this bridge which survived the construction of the deck. Thus no tieplate stress distributions could be drawn.

3.2.2 Coverplated Beams

Two coverplated beam bridges were instrumented: the east approach span of the Columbia-Wrightsville Bridge where the roadway runs parallel to the beams, and the West Chester Bridge which is skewed. In both bridges the beams were composite with the deck and there were no floor beams or girders.

Typical analog traces for gages at the ends of the coverplates of the two bridges are shown in Fig. 26. The vehicles in both cases were five axle semi-trailer (35-2) of unknown weight and speed.

The stress excursions in Fig. 26 take place in approximately 1.0 to 1.5 sec. which corresponds to the time required for a truck to cross the span at about 50 mph (90'). The 90' distance is roughly the span length plus the length of the truck. It would appear then that the loading is wheel dependent since the excursions consist of a number of humps which occur in the time that it takes the entire truck to cross the span. Significant stress reversal occurred at all the gage locations on the West Chester Bridge beams. No stress reversal was observed in the Columbia-Wrightsville coverplated beams.

The maximum live load stress recorded at the ends of the coverplates in the Columbia-Wrightsville Bridge was 2.9 ksi. This was much lower than the design stress of 9.3 ksi. The maximum stress range was 3.0 ksi. At the West Chester Bridge a maximum live load stress of 1.0 ksi and a maximum stress range of 1.5 ksi was recorded. The recorded maximum live load stress was again much lower than the design stress which was 4.3 ksi.

3.2.3 Diaphragms and Diaphragm Connections

Gages were placed on the diaphragms and on the bridge beam webs. At the connections of the diaphragms of the West Chester Bridge, Figs. 12, 17 and 18. The maximum recorded live load stress and stress range did not exceed 1.5 ksi in either case. Figure 27a shows the stress time traces for a gage (29) on the beam flange below a diaphragm connection plate and a gage (28) next to the connection plate on the beam web. Excursions in Fig. 27a occur in 1 to 1.5 sec. which is the time it takes a truck to cross the span at about 50 mph. The time of the excursion is the same as that for the beams at the ends of the coverplates, Fig. 26. There is no discernible difference in magnitude or in the variation of stress with time for the two traces. This was true throughout the recording period. The attachment of the diaphragm connection plate to the beam in this case, therefore, did not significantly alter the magnitude or the variation of stress with time.

3.2.4 Girder Flange Splice

A maximum live load stress of 2.1 ksi was recorded for the flange at the splice on the Columbia-Wrightsville Bridge, Fig. 19a. This maximum live load stress and the maximum stress range of 4.1 ksi were less than the design stress of 6.7 ksi. The ultra violet stress time traces for gage 26 on a flange at a splice and gage 25 some 22 feet away on the same girder near a gusset plate attachment are shown in Fig. 27b. In each instance the stress excursion takes in approximately 3.5 sec. which corresponds to a truck crossing about two spans. This time interval is the same as that for the tieplate

on the same bridge, Fig. 22. The stress excursion of the tieplate also shows the same stress reversal. The similarity between stress variations in girders at all instrumented locations and in the tieplates indicates that the stresses in the girders and the tieplates are related to the stresses in the girder. The relationship is investigated in Chapter 4.

3.2.5 Floor Beam Details

A number of floor beam details were instrumented at the Columbia-Wrightsville and the Interstate Route 81 Susquehanna River Bridges. Gages were placed on the floor beam at the catwalk attachments, Fig. 15, and near knee brackets, Fig. 14. One gage was also placed on a knee bracket, Fig. 14, at the Interstate Route 81 Susquehanna River Bridge.

The maximum recorded stress for a floor beam detail was 1.8 ksi (Gage 22) near a knee bracket on the Columbia-Wrightsville Bridge. This live load stress and the maximum stress range of 2.7 ksi were much smaller than the design stress of 16.2 ksi. The Interstate Route 81 Susquehanna Bridge floor beams had a maximum live load stress of 1.0 ksi and a maximum stress range of 1.0 ksi at a catwalk attachment (Gage 16). The design stress was 13.8 ksi.

3.2.6 Girders and Stringers

Gages were mounted on longitudinal girders, Fig. 16b, and stringer flanges, Fig. 16a, at South Bridge, near gusset plate attachments, Fig. 19b, at the Columbia-Wrightsville and Interstate Route 81 Susquehanna River Bridges; and near a flange splice at the

Columbia-Wrightsville Bridge, Fig. 19a. All recorded stresses and stress ranges were below 4.5 ksi. The maximum recorded values together with the design stresses are listed in Table 3. The measured stresses correspond to the findings from other investigations on longitudinal girders (9, 10, 11, 12).

The stress variations in a girder near a splice and at a gusset plate of the Columbia-Wrightsville Bridge have been shown in Fig. 27. Figure 28 depicts the variation of stress with time for gages on the girders of the Interstate Route 81 Susquehanna River, the Columbia-Wrightsville and South bridges. The duration of each stress excursion is the time required for a truck (the live load) to move across approximately two spans. The girder traces from each of the three bridges is qualitatively the same once the difference in the time scale is accounted for.

The gaged stringer on South Bridge, Figs. 7 and 16a, had a maximum stress of 3.5 ksi and a maximum stress range of 6.0 ksi. The design stress was 23.6 ksi. As was the case in the floor beams the recorded stresses were much lower than the design value.

A point on the flange of a continuous span girder will be subjected to alternating live load bending tensile and compressive stresses as the load moves along the girder. Since the stress at a point in a girder is directly proportional to the moment at the girder cross section, the variation of stress with time is analogous to the influence line for moment at that section. The stress time traces for a girder and a stringer at South Bridge, and the influence line for

moment at the girder section are shown in Fig. 29. The South Bridge stringer is a continuous beam composite with a concrete deck. The stringer and the girder traces are analogous. The girder trace is also analogous to its influence line for moment. Also each trace in Fig. 28 corresponds to the influence line for moment for that particular gage location.

3.3 Evaluation of Fatigue Strength of Tested Details

The 1974 AASHTO Specifications (13) were used in evaluating the fatigue strength of the bridge details under study. Table 4 lists the details studied, their maximum recorded live load stress range, the AASHTO category the detail falls under, and the allowable range of stress (F_{sr}) for that category. The allowable range of stress was taken for over 2,000,000 cycles since the bridges are on arteries which are very heavily traveled or expected to be very heavily traveled. With the exception of the open tieplates at South Bridge, all the details studied had their maximum recorded stress range below the AASHTO allowable range of stress for its category.

While research is in progress to examine the validity of stress range threshold for fatigue failure of these bridge details, some assumptions may be made here so as to enable the evaluation of fatigue strength. By assuming that the allowable stress ranges for high cycle fatigue (over 2,000,000 cycles) are valid, that maximum live load stress ranges in the future will not be more than 20 or 30% of the recorded maximum stress ranges of this study, and that no

deterioration of the bridges by other means will alter the stress pattern at the details, it can be concluded that these bridge details would most probably not be subjected to fatigue failure.

The stress ranges in the tieplates of the South Bridge are higher than the allowable stress range by AASHTO. The cause of these stresses, the listing of their occurrence and the evaluation of the fatigue strength of these tieplates are discussed in the following chapters.

4. STRESS EVALUATION OF TIEPLATES AND TIEPLATE RIVETS BY ANALYTICAL MODEL

4.1 Analytical Model for Tieplates

The open tieplates at South Bridge are subjected to in-plane horizontal bending live load stresses that have not been taken into account in their design. Also rivet failures have been discovered in the connections of the tieplate to the floor beam and the girder. In this section the causes of these horizontal bending stresses are examined through the use of an analytical model. The failure of tieplate rivets will be analyzed using the same model.

The stress excursions for a point on the flange of a girder and for a point on the tieplate of the South Bridge, Figs. 23 and 28, occur in the same length of time. The stress versus time traces also have the same shape. These observations lead to the assumption that the variation of stress in the tieplate with time is directly related to the variation of stresses in the girder flanges.

The live load stress distribution pattern in the South Bridge tieplate, Fig. 23, has indicated that the plate was subjected to horizontal, in-plane bending. A horizontal displacement of the tieplate relative to its ends, or to some points along the tieplate, will reduce such a bending stress pattern. Figure 30 shows the top view of a tieplate in the South Bridge. Superimposed on the plate is

a possible centerline shape of horizontal deflection assuming the stringers serve as supports. From mechanics of material it can be derived that, for a given configuration and geometry of the assembly, the horizontal bending stress σ is proportional to the displacement ΔH, that is $\sigma = \alpha(\Delta H)$.

Since there is no external load being applied at this bridge detail, the horizontal displacement and the bending stresses must be induced by forces or displacements from other components of the bridge structure.

Consider a section of a continuous girder in bending, Fig. 31. Under positive moment by live load, the top flange compresses and a point (a) on the top flange displaces horizontally along the length of the girder, Fig. 31a. This displacement (ΔH_1) equals the slope of the girder at that point (θ_1) multiplied by the centroidal distance between the point and the neutral axis (c), $\Delta H_1 = c\ \theta_1$. The tieplates are attached to the girder flanges and undergo the same displacements. The horizontal displacement (ΔH_1) then is the cause of the in-plane, horizontal bending of the tieplate and the corresponding bending stresses in the plate. The relationship between the tieplate stresses and the girder slope (rotation) is $\sigma = \alpha\ (c\ \theta_1) = \beta\ \theta_1$, where β is a proportional constant depending upon the configuration and geometry of the stringer-floor-beam-tieplate system and the girder.

Since South Bridge is a continuous girder bridge, reversal of curvature in the girder occurs as a truck moves from one span to the next, Fig. 31b. The reversal of curvature displaces the same

point (a) on the top flange in the opposite direction. This horizontal displacement (ΔH_2) produces horizontal bending stresses in the plate opposite to those induced by the displacement ΔH_1. Reversal of direction in cross-sectional rotation (or slope) thus brings about stress reversal in the tieplate.

The time variation of stress in the tieplate and the influence line for the scope of the girder at the point of the tieplate should be analogous. A comparison is made in Fig. 32 for two different tieplates in South Bridge. In both cases the analog record of stress stresses and the influence line for girder rotation are comparable. This agreement confirms the relationship of direct proportionality between the tieplate stresses and the girder slope. Also since the girder slope at a point is directly proportional to the stresses at the top flange of the girder, the girder stresses are directly proportional to the tieplate stresses, as has been assumed at the onset of this analysis.

In order to evaluate the constant, β, which relates the tieplate stress to the girder rotation an examination of the bridge structure is necessary. The floor beam, tieplate and bracket system is a transverse, continuous beam which supports the stringers, and is in turn supported by the girders. Any truck load on the bridge deck is transmitted through this system to the girders, resulting in bending moments, shearing forces, vertical deflections, and rotations of the girders. The rotation of a girder induces a horizontal, out-of-plane displacement in the transverse continuous beam.

The out-of-plane displacement is restrained by the stringers which are composite with the concrete deck and thus subject to little horizontal displacement. Therefore, it can readily be assumed that the out-of-plane displacement of the transverse continuous beam takes place primarily within the region bounded by the first inboard and the first outboard stringers. Figure 33 shows schematically the model representing the portion of a floor beam-tieplate-bracket system between the first inboard and the first outboard stringers. These stringers are assumed to act as elastic supports to the transverse beam. The beam is subjected to a horizontal, out-of-plane displacement ΔH at the centerline of the girder. The moment of inertia of the beam is segmentally constant along the length to take account for the different stiffnesses of the floor beam, the tieplate, and the outrigger bracket in the direction of the out-of-plane displacement ΔH. The beam is most flexible at the girder where it consists of the tieplate alone.

The magnitude of the horizontal bending stresses in the tieplate due to the displacement ΔH depend on the length and rigidity of the segments of this beam. The stresses also depend on the restraints provided by the elastic supports (stringers) against displacement and rotation. The more rigid the connections of the stringers to the floor beam the higher the tieplate stresses.

Determining the amount of support restraint at individual tieplates of the South Bridge is quite difficult. At the locations of failed rivets in the stringer to the floor beam connection, the restraint definitely is less than at locations where the rivets are

intact. In order to explore the possible magnitudes of the bending stresses in the tieplates, the boundary conditions of the model in Fig. 33 were first considered as simply supported and then rigidly fixed, Fig. 34. The actual support conditions lie somewhere between these extremes.

Large horizontal displacements cause high stresses in the tieplates. With high stresses and a large number of repeated load applications, fatigue cracking could occur at susceptible details on the tieplate. While no cracks have been observed in the South Bridge tieplates, the same phenomenon has produced fatigue cracks in the tieplates of the Lehigh Canal and Allegheny River Bridges (12). South Bridge and Lehigh Canal and the Allegheny River bridges have experienced rivet failures at the stringer-floor beam connections and at the tieplate girder joints as reported in Chapter 1. The cause of these rivet failures is examined in the next section.

4.2 Analysis of Rivet Failures

A histogram of rivet failures versus rivet location for the South Bridge is shown in Fig. 35. More failures occurred at piers than towards the center of the spans. From the model used for the tieplate stress analysis, it was found that large displacements (ΔH) of the girder flange generate high shearing forces and moments at the tieplate rivet joints. Since ΔH is directly proportional to girder slope which is higher at the piers, Fig. 35, it was concluded that rivet failures were caused by the same out-of-plane displacement which induced horizontal bending stresses in the tieplate. This

permits the analysis of rivet failures using the same analytical model as described by Figs. 33 and 34.

The horizontal displacement ΔH at the top flange of the girder is transmitted to the tieplate through a number of filler plates. If the rivets have sufficient clamping force to induce a large amount of friction between each of the plates, the connection behaves as a monolithic elastic block and there is little live load stress in the rivets. However, when friction is insufficient, slippage between the plates takes place when ΔH is introduced by the live load on the bridge. The slippage causes differential deflection of the rivet shank, Fig. 36, and bearing of one side of the rivet head against the tieplate or the girder flange. This phenomenon is identical to that which has been observed in riveted lap joints (14). Under repeated truck loads and the corresponding ΔH's, the stress in the shank may trigger fatigue cracking and eventual rivet failure.

The tieplate rivet failures in the South Bridge could be separated into two distinct types: those that failed in the tieplate to girder connections and those that failed at the stringers. The failures at the stringers were through the shank. While no information was available as to the mode of failure of the rivets in the girder connections, rivet failures at similar locations at the Lehigh Canal Bridge were by fatigue under the rivet head.

To obtain an estimate of the stresses just under the rivet head as caused by the differential displacement between the two ends of a rivet, the rivet is considered as a beam subjected to bearing

forces (q) from the plates, Fig. 37. The dimensions t_1, t_2, t_3 are the thicknesses of the tieplate, shim plates, and girder flange respectively. The bearing forces may be assumed to have any configuration of distribution, Fig. 37a, b, and etc., so long as it is constant with the plate arrangement and is in the self-equilibrium in the direction of these forces. These forces produce the differential displacement ΔH and the moments (M_1 and M_2) under the rivet heads. The magnitudes of M_1 and M_2 also depend upon the restraint to rotation of the rivet heads when they bear on the surface of the tieplate and the girder flange. If the rivet heads are fixed (not able to rotate at all) a value of $\Delta H = 0.0001$ in. would produce a bending stress of 30 ksi in a 2 in. long rivet of a 7/8 in. diameter rivet.

In the lateral direction along the length of the tieplate, (Section A-B) of Fig. 36, the expansion and contraction of the tieplate induced by its horizontal bending will also introduce differential displacements to the rivets. Again, bending stresses are induced in the shank. The result is that the rivets are subjected to bending stresses in two perpendicular directions as shown in Fig. 38. The orientation of principal (highest) stresses in the rivet shank are also shown in the figure. These orientations, and the directions fully agreed with the crack patterns of rivets in the Lehigh Canal Bridge.

Another observation from rivet failure under its head (at the Lehigh Canal Bridge) was that the cracks drove up into the rivet head. This phenomenon is also consistent with the analytical model.

Under the rivet head, small shearing stresses develop due to bearing of the rivet head on the tieplate. The combination of the bending stresses and the shear stresses produces the stress state at element a shown in Fig. 39. The crack grew perpendicular to the line of principal stress and drove into the rivet head.

The failure of rivets at the stringers of the South Bridge were through the body of the shank indicating a shear failure. The stringers serve as supports for the beam model of Fig. 33. The horizontal displacement ΔH at the girder induces moment and shear (reactions) at the stringers (supports). The magnitudes of these moments and shears depend on the effectiveness of the stringer-floor beam connection. In other words, the more rigid the connection, the higher the moment and shear forces to be distributed among the rivets at this connection for a given ΔH. Also, the moments and shears at the two supports (stringers) depend on their distance from the girder. Higher moment and shear forces are induced in the support which is closer to the girder. Most of the rivet failures at the South Bridge were at the first inboard stringer which is quite close to the girder. This agreement is further configuration to the validity of the assumed analytical model.

4.3 Stress Estimates for South Bridge Tieplates

Stresses were estimated for the tieplates over pier 20 of South Bridge using the analytical mode. A 72-kip truck load on one girder was used to approximate the maximum live load experienced by

the bridge. The actual dimensions of the bridge were utilized in estimating the rotation of the girder and computing the tieplate stresses.

The computed stresses of the pier 20 tieplate at the inboard edge of the girder top flange were 2.6 ksi for the simply supported case and 7.3 ksi for the fixed case of Fig. 34. The stresses for the outboard side were 4.5 ksi (simple supports) and 24.5 ksi (fixed ends). The maximum recorded stress for the two tieplates at this location was 7.7 ksi, Fig. 24. Rust particles between the stringers and the east tieplate at pier 20 were observed during field inspection. This indicates sliding between these two components which would reduce the restraint at the support of the model beam and explain why the stresses in the east tieplate were lower than those in the west tieplate.

The computed values of shear stress in the rivets at the first inboard stringer at pier 20 were 2.5 ksi for the simply supported case and 3.5 ksi for the fixed condition. Assuming that the actual shear stresses in the rivets were half way between these values, in the order of 15 to 20 ksi, this would account for the numerous rivet fatigue failures encountered at South Bridge.

To estimate the stresses in rivets that failed under its head, the bearing force configuration of Fig. 38a was assumed. For a 7/8" diameter rivet at pier 20 with a length of 3-3/16" (1" of shim plates), a differential displacement of 0.01 in. would produce stresses of 40 ksi if the head were rigidly held in place against

rotation. Inspection of the rivets revealed that many of the rivets were not tightly clamped to the plates. This condition would permit very slightly rotation of the rivet heads which would reduce the stresses in the rivets at the tieplate to girder connections.

4.4 Discussion on Tieplate Arrangement

The examination of tieplate stresses and rivet failure through the use of an analytical model allows a rational explanation of the causes of tieplate and rivet cracks. The primary cause is the differential displacement ΔH along the top flange of the girder. Consequently, the prevention of tieplate and rivet failures is best accomplished by reducing this differential displacement.

In the Columbia-Wrightsville and the Interstate Route 81 Susquehanna River Bridges the horizontal differential displacement is very small because the top flange of the girder and tieplates are embedded in the concrete deck. The girders and the deck behave compositely little relative displacement at the tieplates would be expected. The recorded horizontal bending stresses in the tieplates were very low at the Columbia-Wrightsville Bridge, in the order of 1.0 ksi as compared to 11.0 ksi at the South Bridge, where the "open" tieplate system is used.

When the tieplates connecting the floor beams and outrigger brackets to the girder flanges are not embedded, and the stringers are supported thereon, the horizontal displacement of the girder flange is transmitted to the tieplates. This transmission can be

prevented by removing the rivets or bolts connecting the tieplate to the girder flange. In other words, if the tieplate connects the outrigger bracket to the floor beam but "rides free" over the girder flange, the horizontal bending of the tieplate and the corresponding stresses would be reduced. This configuration, however, requires analysis of the web connections between the girder and the floor beam and the girder and the outrigger bracket since the girder deflection produces out-of-plane web deflection in the floor-beam and outrigger bracket.

If the tieplate is connected to the girder flange, the horizontal displacement due to live load induces stresses in the tieplate. By using the analytical model, it can be shown that (1) for given distances between the girder and the two stringers to each side, a narrow tieplate has lower bending stresses, (2) the longer the distance between the girder and a stringer, the lower the bending stresses in the tieplate, and (3) the more rigid the connections between the stringer and the floor beam, the higher the stresses in the tieplate and in the connectors at the stringer. The effect of the tieplate width has been demonstrated in a bridge test (15). The influence of the distance between the first inboard or outboard stringer and the girder is confirmed by comparing the Lehigh Canal Bridge and the Allegheny River Bridge (12). When this distance is very short, as in the case of the South Bridge, shear rather than bending governs and the rivets at the stringer encounter failure. The failure of rivets at the stringer, however, releases the restraint to the floor

beam at this point and greatly increases the distance between the support points of the model beam which in turn greatly decreases the stresses in the tieplate.

For existing bridges with "open" tieplates connecting the outrigger brackets and floor beams to the girder, the stresses induced by live load on the deck should be evaluated and to ensure that the system is flexible enough to prevent fatigue failures.

5. CORRELATION WITH FATIGUE TEST RESULTS

5.1 Stress Range Occurrences

In Chapter 3 it has been summarized that all details of this study, except the tieplates at the South Bridge, have low recorded stresses. By comparing the maximum stress range recorded for the details with the corresponding allowable stress range from the AASHTO Specifications it is concluded that these details will not fail in fatigue. The open tieplates at the South Bridge were found to have high stress ranges due to live load. In order to evaluate the fatigue strength of these tieplates, the stress history of each must first be estimated.

The detailed stress range occurrence data for five gages on the South Bridge tieplates with highest recorded stresses are listed in Table 5. These data were compiled from the analog traces, Fig. 20, taken during field testing. An arbitrary cutoff (minimum) value of 2.0 ksi was used. All five gages were along the plate edges. Table 5 shows the stress range levels and the frequency of occurrence of live load stresses between these levels. The recording time was from 1 to 2 hours.

The stress range occurrence data were also plotted as histograms, depicting the percentage of frequence of occurrence between the stress range levels. Examples are shown in Figs. 40 to 44. All the

tieplates experienced stress ranges above 5 ksi, the allowable stress range of AASHTO Category E details for lives over 2,000,000 cycles. The frequency of occurrence of lower stresses was higher.

5.2 Traffic Records

The histograms of Figs. 40 to 44 are from measurements made in a very short duration of time. The validity of these distributions as representative of the stress range occurrences throughout longer periods of bridge traffic must be established. This is done indirectly through comparisons of traffic records.

Truck traffic counts were taken during the inservice field testing of the Columbia-Wrightsville, West Chester and South Bridges. There was no appreciable truck traffic over the Interstate Route 81 Susquehanna River Bridge at the time of testing. Tables 6 to 8 give the truck counts by type obtained for the three bridges. The distribution of trucks were comparable for all three bridges. At each bridge five-axle semi-trailers were most frequently observed and two-axle trucks had the second highest percentage. These observations agree very well with the results of a twenty-four hour traffic count near the bridge sites. These counts were obtained from PennDOT. The twenty-four hour count from PennDOT for the Columbia-Wrightsville and South Bridges are copied in Tables 9 and 10. The consistency of the distribution of truck type between truck counts taken in very short durations and in twenty-four hour periods indicates that the truck counts at the bridges are representative of the normal traffic flows over the bridges. Therefore, the stress range frequency distribution

of Table 5 for the South Bridge tieplates can be considered as representative of the live load stress range spectrum that the bridge has been subjected to during the years of its existence.

5.3 Laboratory Fatigue Test Results

Laboratory fatigue test results of beams and girders indicate that stress range is a primary controlling factor for fatigue strength (5, 6). An increase in applied stress range leads to a decrease in fatigue life. Based on laboratory test results, the 1974 AASHTO Specifications (13) divide bridge details into five categories (A to E). Each category defines permissible stress ranges according to the number of anticipated stress cycles. There is no specific category for riveted joints subjected to bending in its own plane, as in the case of the South Bridge tieplates. Fatigue test results of riveted joints in tension indicates that AASHTO Category E would be appropriate for such joints when stresses are computed on the gross area. It is assumed here that tieplate is also represented by Category E with stress ranges computed at the edge of the rivet hole (16) where it is assumed cracks would originate.

To correlate the tieplate stress data at South Bridge with laboratory fatigue test results, the total number of trucks that c crossed the bridge in the thirteen-year period (1960-1973 from its opening to the time of the field study) must be estimated. The average daily traffic (ADT) counts from PennDOT for each year of the bridge life is plotted in Fig. 45. Because only trucks cause

measurable stresses, the average daily truck traffic (ADTT) is first evaluated as a constant percentage of the ADT. This percentage was lower for weekends than for weekdays (14% versus 8%). The total volume of truck traffic from 1960 to 1973 was then summed. The computed amounts for South Bridge were 27.7 million trucks northbound and 28.0 million trucks southbound.

5.4 Correlation

The field measurements and traffic data records provided stress range spectra at the tieplates and the estimated number of trucks which caused these spectra. Fatigue test results from laboratories are, on the other hand, for constant amplitude stress ranges. To correlate field data and laboratory results, either a Root-Mean-Square (RMS) equivalent constant amplitude stress for a stress spectrum is computed, or Miner's Hypothesis is employed.

5.4.1 Root-Mean-Square Estimates

The Root-Mean-Square stress range (5, 17, 18) replaces a spectrum of stress ranges by a single value which is considered equivalent to a constant cyclic stress range. The Root-Mean-Square stress range and the total number of stress cycles corresponding to the spectrum then can be used to compare with the appropriate S-N curve.

The Root-Mean-Square stress range is defined as

$$S_{rRMS} = (\Sigma \alpha_i S_{ri}^2)^{1/2}$$

where α_i is the frequency of stress range S_{r1}. The RMS stress ranges for the stress range histogram of five South Bridge tieplates, Figs. 40 to 44, were computed and are listed in Table 11. These values were then adjusted to the edges of the rivet holes for which the constant cycle fatigue data are assumed to apply. Also listed in the table are the estimated number of trucks corresponding to the stress values.

Assuming that one truck caused one stress range excursion, the number of fatigue cycles at the tieplates was equal to the number of trucks that crossed the bridge (northbound or southbound depending on the gage location). These cycle numbers and the corresponding S_{RMS} values at the edge of the rivet holes are plotted in Fig. 46, where the line of allowable stresses of Category E is also shown. This line is the 95% confidence limit that no fatigue failure would occur. All the data points are below the line. None of the tieplates were cracked at the time of the test.

5.4.2 By Miner's Hypothesis

The combination of Miner's Rule (19) and constant cycle data (5) gives an equivalent stress range S_{rMiner}(16) which is defined as $S_{rMiner} = (\Sigma \alpha_i S_{ri}^3)^{1/3}$ where α_1 is the frequency of occurrence of stress range S_{ri}.

The number of load cycles corresponding to this value is the same as for the Root-Mean-Square stress range presented earlier. The S_{rMiner} values for the tieplates are plotted in Fig. 47 which is similar to Fig. 44. Here two points are above the cutoff level corresponding to the 95% confidence limit for Category E.

Since there is little data on fatigue tests of riveted or bolted plates subjected to in-plane bending, the applicability of AASHTO Category E is uncertain. There is good correlation in that the stress magnitude and history conditions of the tieplates lie near or below the cutoff level corresponding to the 95% confidence limit for Category E. None of these tieplates have developed cracks. It is doubtful, however, that the implication of the horizontal line portion of the S-N curve is valid. In other words, it is likely that these tieplates will experience fatigue cracking if the present stress levels persist.

6. SUMMARY AND CONCLUSIONS

The analyses of the results of the field tests of the four bridges described herein lead to the following summary and conclusions:

1. The live load stresses recorded in the main longitudinal girders were lower than the design values, as was observed by other investigators on other bridges. The live load stresses did not exceed 3 ksi in the bridges of this study.

2. Live load stresses in floor beams and stringers were less than 50 % of the design values.

3. The open tieplates at South Bridge had relatively high, being above the AASHTO allowable stress for Category E details for more than 2,000,000 cycles.

4. The stresses on the tieplates of South Bridge were in-plane horizontal bending stresses with the maximum value in the order of 10 ksi. These stresses were similar in magnitude and distribution to those encountered in earlier field tests on other bridges with open tieplates.

5. Interstate Route 81 Susquehanna River Bridges had much lower stresses with the value in order of 1 ksi. The tieplates and girder flanges of these bridges were encased in concrete.

6. Magnitude of horizontal bending stresses in the tieplate is found to be related to the stresses in the top flange of the girder.

7. An analytical model was developed to evaluate bending stresses in tieplates and stresses causing rivet failures. Field observations on plate failures at other bridges and on the failure mechanisms of the rivets confirmed the adequacy of the model.

8. Based on the model, it would be most effective to control tieplate or rivet failure if the tieplate is embedded in the concrete deck. This is borne out at the Columbia-Wrightsville and the Interstate Route 81 Susquehanna River Bridges.

9. Unbolting the tieplates from girders for existing bridges would permit the tieplate to be free from the horizontal bending preventing tieplate and rivet failures.

10. Reducing the width of tieplates would also reduce the bending stresses in these plates.

11. Truck counts were taken and found to be compatible with PennDOT loadometer survey results. Five-axle semi-trailer was the most frequent truck on the bridges.

12. Stress range history for the details of the bridges were obtained.

13. There appears to be little fatigue data on riveted or bolted plates subjected to in-plane bending for comparison with the tieplate stresses.

14. The Root-Mean-Square stress, S_{rRMS}, range and an equivalent stress range, S_{rMiner}, by the Miner's Hypothesis together with an estimated traffic volume over South Bridge for the period 1960-1973 provided good correlation with laboratory fatigue test results of riveted joints in tension (AASHTO Category E).

TABLE 1

RECORDED STRESSES IN TIEPLATES

Columbia-Wrightsville Bridge

Gage	Highest Stress Range Level (By FHWA System) (ksi)	Maximum Live Load Stress (By Analog Traces) (ksi)
7	1.2	0.6
8	1.5	0.5
9	1.5	0.3
10	1.5	0.2
11	1.5	0.5
12	1.5	0.4
16	-	0.1
17	-	0
18	-	0
19	-	0
20	0	0.1
21	-	0.1
23	1.5	0.3
24	1.5	0.3
27	1.5	0.8
28	1.5	1.0
29	0.6	0.2
30	0.6	0.2

TABLE 1 (continued)

RECORDED STRESSES IN TIEPLATES

Interstate Route 81 Susquehanna River Bridge

Gage	Highest Stress Range (By Analog Traces) (ksi)	Maximum Live Load Stress (By Analog Traces) (ksi)
8	0.1	0.1
9	0.2	0.2
10	0.5	0.2
13	0.5	0.5

South Bridge

Gage	Highest Stress Range (By Analog Traces) (ksi)	Maximum Live Load Stress (By Analog Traces) (ksi)
11	8.5	6.0
12	4.0	3.2
13	7.5	5.2
14	7.0	4.0
15	4.0	2.5
16	6.0	3.0
17	10.0	8.5
18	4.0	2.5
19	9.0	6.0
20	11.5	9.5
21	3.0	2.5
22	7.7	7.0
23	7.0	5.5
24	3.0	2.5
25	13.0	11.0

TABLE 1 (continued)

RECORDED STRESSES IN TIEPLATES

South Bridge (continued)

Gage	Highest Stress Range (By Analog Traces) (ksi)	Maximum Live Load Stress (By Analog Traces) (ksi)
26	13.5	10.5
27	3.0	3.0
28	10.7	8.0
29	13.0	9.0
30	3.0	2.7
31	10.0	6.5
32	10.0	6.0
33	2.0	1.5
34	9.0	5.0
39	13.5	10.5
40	9.0	5.5
42	8.0	7.2
43	4.5	2.0
44	12.0	10.2
46	12.5	7.7
47	2.0	1.5
48	11.2	5.7
49	10.5	5.5
50	2.5	2.0
51	13.3	6.7
54	4.7	2.5
55	1.0	0.7
56	5.0	3.0
57	9.0	5.0
58	1.0	0.5
59	9.0	4.7

TABLE 1 (continued)

RECORDED STRESSES IN TIEPLATES

South Bridge (continued)

Gage	Highest Stress Range (By Analog Traces) (ksi)	Maximum Live Load Stress (By Analog Traces) (ksi)
60	11.0	9.7
61	4.5	4.0
62	8.0	7.2
63	12.0	10.0
64	4.5	2.7
65	9.0	8.2
66	11.0	10.5
67	-	-
98	9.0	5.0
99	14.0	10.5

TABLE 2

STRESSES IN COVERPLATED BEAMS AND DIAPHRAGMS

West Chester Bridge

Gage	Highest Stress Range Level (FHWA System) (ksi)	Maximum Live Load Stress (By Analog Traces) (ksi)	Live Load Design Stress (ksi)
1	1.50	0.75	6.5
2	1.50	2.00	6.5
3	1.50	1.20	6.5
4	1.50	1.10	6.5
5	1.50	1.00	6.5
6	1.50	1.00	6.5
7	0.45	1.11	6.5
8	0.15	-	6.5
9	-	1.20	6.5
10	1.50	1.50	8.8
11	1.10	0.45	-
12	1.50	1.35	-
13	0.60	-	8.7
14	1.50	-	7.5
15	0.15	-	7.5
16	-	-	7.5
17	1.50	1.40	7.5
18	1.5	-	7.5
19	1.5	-	7.5
20	1.50	-	7.5
21	-	-	7.5
22	-	-	7.5
23	1.5	-	7.5
24	-	-	7.0
25	-	-	7.0
26	1.50	-	7.0

TABLE 2 (continued)

STRESSES IN COVERPLATED BEAMS AND DIAPHRAGMS

West Chester Bridge (continued)

Gage	Highest Stress Range Level (FHWA System) (ksi)	Maximum Live Load Stress (By Analog Traces) (ksi)	Live Load Design Stress (ksi)
27	-	1.50	-
28	1.50	0.90	7.5
29	1.5	0.95	7.0
30	0.9	-	7.0

Columbia-Wrightsville Bridge

Gage	Highest Stress Range Level (FHWA System) (ksi)	Maximum Live Load Stress (By Analog Traces) (ksi)	Live Load Design Stress (ksi)
(1)	3.0	2.9	9.3
2	2.1	2.0	9.3
3	2.6	2.5	9.3
4	2.4	2.4	9.3
5	2.0	1.0	9.3
6	2.1	2.0	9.3

TABLE 3

STRESSES IN GIRDERS, FLOOR BEAMS AND STRINGERS

Columbia-Wrightsville Bridge

Gage	Highest Stress Range Level (FHWA System) (ksi)	Maximum Live Load Stress (By Analog Traces) (ksi)	Live Load Design Stress (ksi)
13	1.5	0.9	16.2
14	1.5	1.2	16.2
15	1.5	1.2	16.2
22	2.7	1.75	16.2
25 NEAR GUSSET	4.1	2.8	4.33
26	4.1	2.1	6.70

Interstate Route 81 Susquehanna River Bridge

Gage	Highest Stress Range Level (FHWA System) (ksi)	Maximum Live Load Stress (By Analog Traces) (ksi)	Live Load Design Stress (ksi)
1	0.7	0.7	1 .8
2	0.5	0.5	13.8
3	1.2	1.2	-
4 (Typical Panel)	3.0	2.4	13.8
5	2.5	2.1	7.0
6	1.7	1.7	7.0
7	2.5	1.9	7.0
9	0.2	0.2	7.0
11	0.7	0.7	13.8
12	0.5	0.5	13.8
14	0.7	0.7	13.8
15	0.7	0.7	13.8
16	1.0	1.0	1.0

TABLE 3 (continued)

STRESSES IN GIRDERS, FLOOR BEAMS AND STRINGERS

South Bridge

Gage	Highest Stress Range Level (FHWA System) (ksi)	Maximum Live Load Stress (By Analog Traces) (ksi)	Live Load Design Stress (ksi)
GIRDER – 35 (BOTT?)	2.5	1.5	11.7
GIRDER – 36 (TOP)	3.0	1.5	11.7
STRINGER – 45	6.0	3.5	23.6
GIRDER – 52 (TOP)	2.0	1.0	6.5

TABLE 4

COMPARISON OF MAXIMUM RECORDED STRESS RANGES

WITH ALLOWABLE AASHTO VALUES

Detail	AASHTO Category	$S_{Rmax.}$ (ksi)	F_{SR} (ksi)
Open Tieplates	E	11.0	5.0
Coverplated Beams	E	3.0	5.0
Diaphragm Connection to Beam	C	1.5	10.0
Catwalk Attachment to Floor Beam	E	1.0	5.0
Knee Bracket Attachment to Floor Beam	E	2.7	5.0
Girder	B	3.0	16.0
Girder Flange Splice	E	4.1	5.0
Gusset Plate Attachment to Floor Beam	E	3.0	5.0
Stringer	B	16.0	6.0

TABLE 5 SOUTH BRIDGE

STRESS RANGE OCCURRENCES IN TIEPLATES

Gage	32	39	44	51	60
Stress Range					
11.0	0	1	2	7	1
10.0	1	2	4	5	1
9.0	0	3	4	2	2
8.0	1	6	10	14	10
7.0	6	11	16	10	12
6.0	9	15	19	34	27
5.0	23	18	32	26	29
4.0	33	28	51	49	57
3.0	49	62	84	63	84
2.0	84	82	30	55	105
Total	206	228	252	~~275~~ 265	328

TABLE 6

WEST CHESTER BRIDGE TRAFFIC COUNT DATA

Vehicle Type	Friday 6/1/73 31 min.	Monday 6/4/73 30 min.	Total Traffic	Total Traffic (%)
B	0	0	0	0
2	12	11	23	23.4
3	6	3	9	9.2
2S-1	4	0	4	4.1
4	0	13	13	13.3
2S-2	3	0	3	3.1
3S-2	15	31	46	46.9
	Σ 40	Σ 58	Σ 98	

TABLE 7

COLUMBIA-WRIGHTSVILLE BRIDGE TRAFFIC COUNT DATA

	Friday 6/22/73 45 min.	Monday 6/25/73 61 min.		Tuesday 6/26/73 96 min.		Wednesday 6/27/73 78 min.		Total Traffic		Total Traffic (%)	
	West	East	West	East	West	East	West	East	West	East	West
Bus	1	1	0	0	0	1	0	2	1	1.28	0.40
2D	17	14	12	19	26	20	25	53	80	33.98	32.13
3	2	2	2	1	3	0	0	3	7	1.92	2.81
2S-1	2	6	3	1	8	5	9	12	22	7.69	8.84
2S-2	14	6	5	1	23	9	11	16	53	10.26	21.29
3S-2	31	24	14	16	23	30	18	70	86	44.87	34.53
Total	67	53	36	38	83	65	63	156	249	100.00	100.00

TABLE 8

SOUTH BRIDGE TRAFFIC COUNT DATA

	Thursday 8/9/73		Friday 8/10/73		Sunday 8/12/73		Monday 8/13/73		Thursday 8/16/73		Total Traffic		Total Traffic (%)	
	East	West	East	West	East	West	East	West	East	West	East	West	East	West
Bus	5	11	3	2	2	4	2	3	6	5	18	25	2.09	2.91
2D	87	79	34	26	3	3	30	22	17	38	171	168	19.82	19.56
3	64	22	9	10	1	0	7	7	15	10	96	49	11.12	5.70
2S-1	16	16	10	7	5	4	4	3	3	9	38	39	4.40	4.54
2S-2	85	67	12	16	11	5	17	28	19	19	144	135	16.69	15.72
3S-2	158	224	60	48	44	28	59	30	75	113	396	443	45.89	51.57
Total	415	419	128	109	66	44	119	93	135	194	863	859	100.00	100.00

TABLE 9

PENNDOT TRAFFIC COUNT DATA

FOR SITE NEAR COLUMBIA-WRIGHTSVILLE BRIDGE

Tuesday 1/23/74 - 24 hours

	East	West	East (%)	West (%)
B	5	6	0.41	0.47
2D	333	341	27.18	26.47
3	32	45	2.61	3.49
2S-1	65	72	5.31	5.59
2S-2	188	203	15.35	15.76
3S-2	602	621	49.14	48.21
Total	1225	12.88	100.00	100.00

TABLE 10

PENNDOT TRAFFIC COUNT DATA

FOR SITE NEAR SOUTH BRIDGE

Thursday 6/7/73 - 24 hours

	East	West	East (%)	West (%)
B	98	110	1.65	1.97
2D	1417	1282	23.80	23.00
3	240	226	4.03	4.06
2S-1	382	319	6.41	5.73
2S-2	939	805	15.68	14.44
3S-2	2884	2831	48.43	50.80
Total	5955	5573	100.00	100.00

TABLE 11

CORRELATION OF STRESS AND CYCLE DATA BY ROOT-MEAN-SQUARE ESTIMATES AND MINER'S HYPOTHESIS (SOUTH BRIDGE TIEPLATES)

Gage	Adjusted S_{rRMS} at Rivet Hole	Adjusted S_{rMiner} at Rivet Hole	N Stress Cycles x 10^6	AASHTO S_r at N (Category E)
32	3.87	4.15	28.0	5.0
39	4.31	4.74	28.0	5.0
44	4.92	5.30	28.0	5.0
51	4.96	5.43	28.0	5.0
60	3.91	4.61	28.0	5.0

Fig. 1 Columbia-Wrightsville Bridge

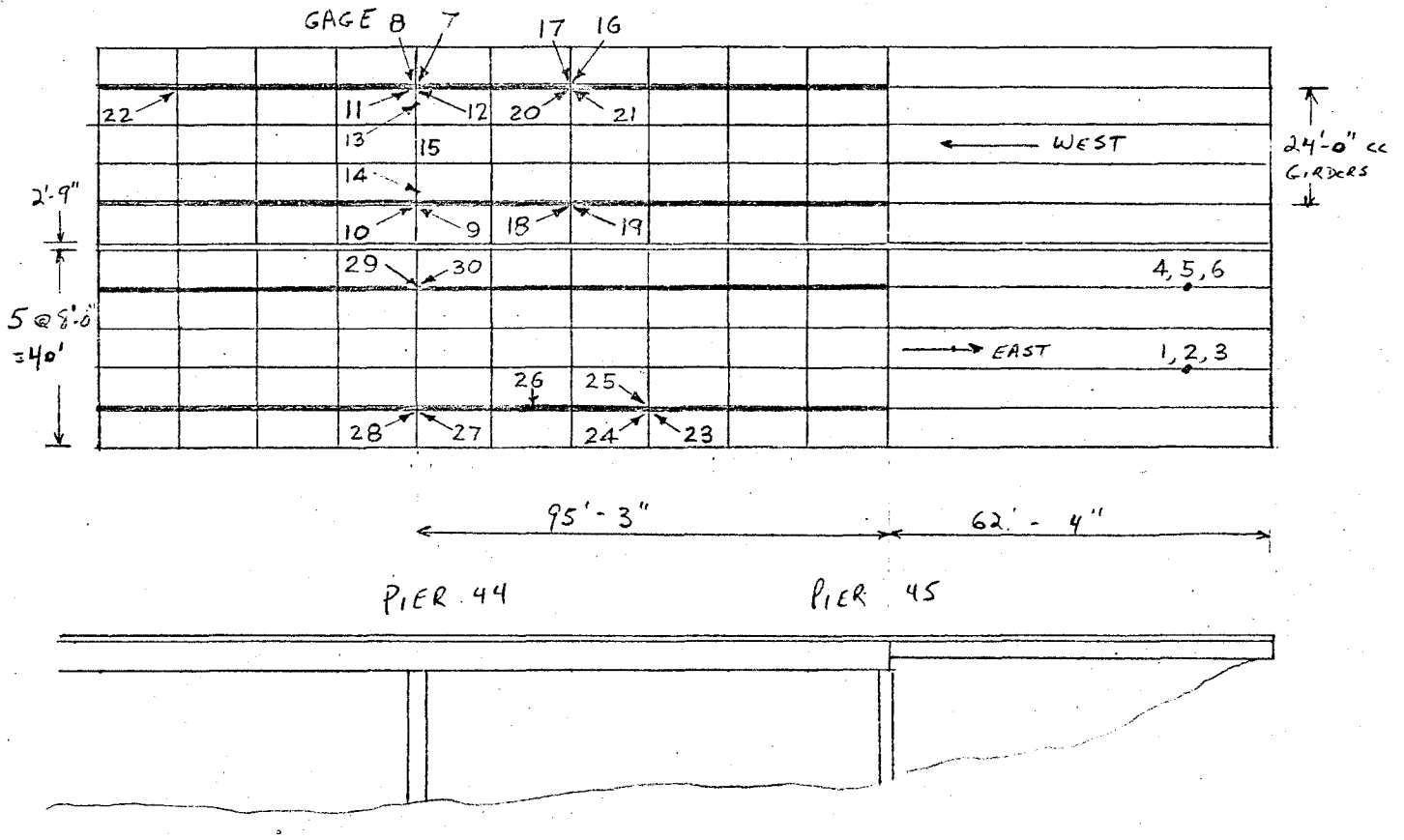

Fig. 2 Plan and Elevation of Columbia-Wrightsville Bridge

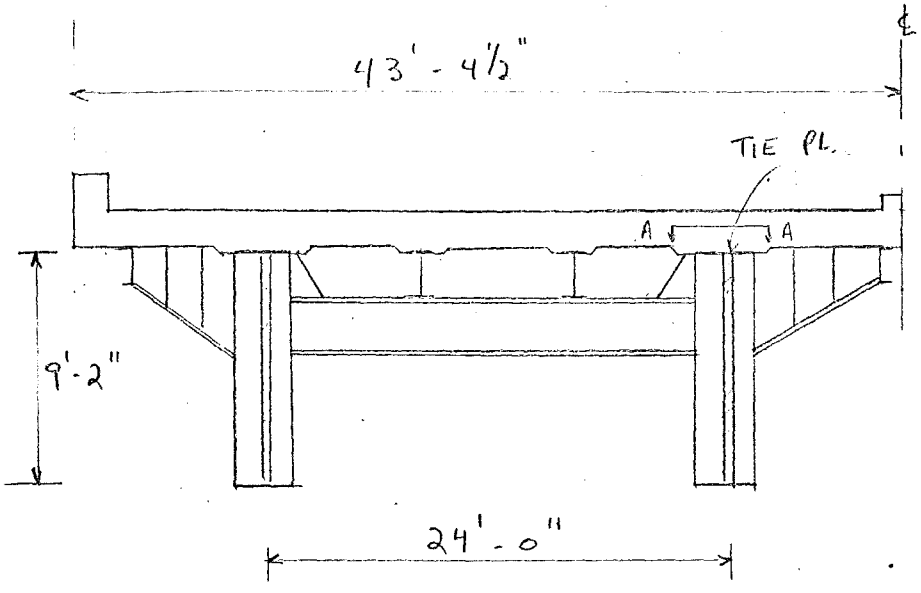

Fig. 3a Cross Section of Columbia-Wrightsville Bridge

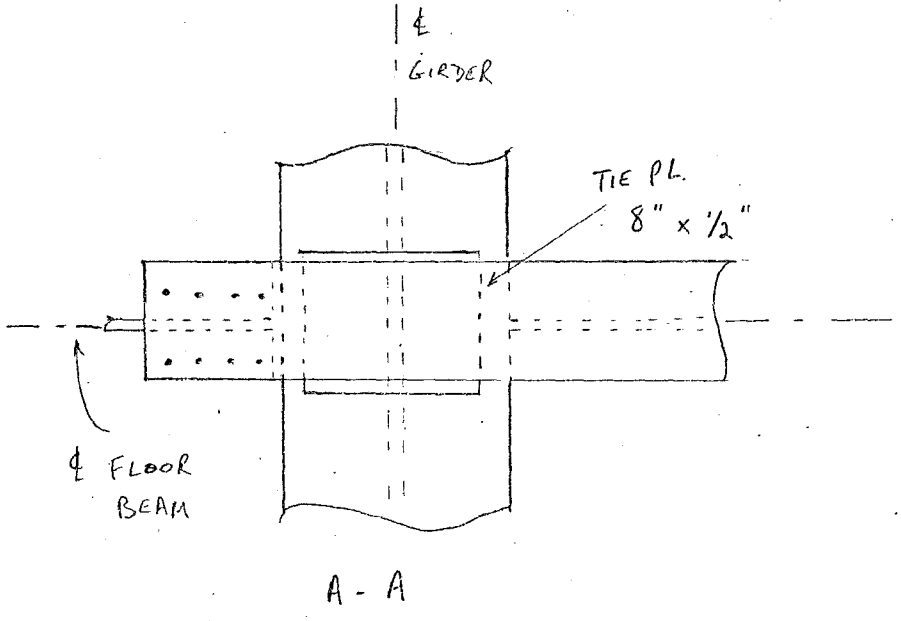

Fig. 3b Tieplate Detail at Columbia-Wrightsville Bridge

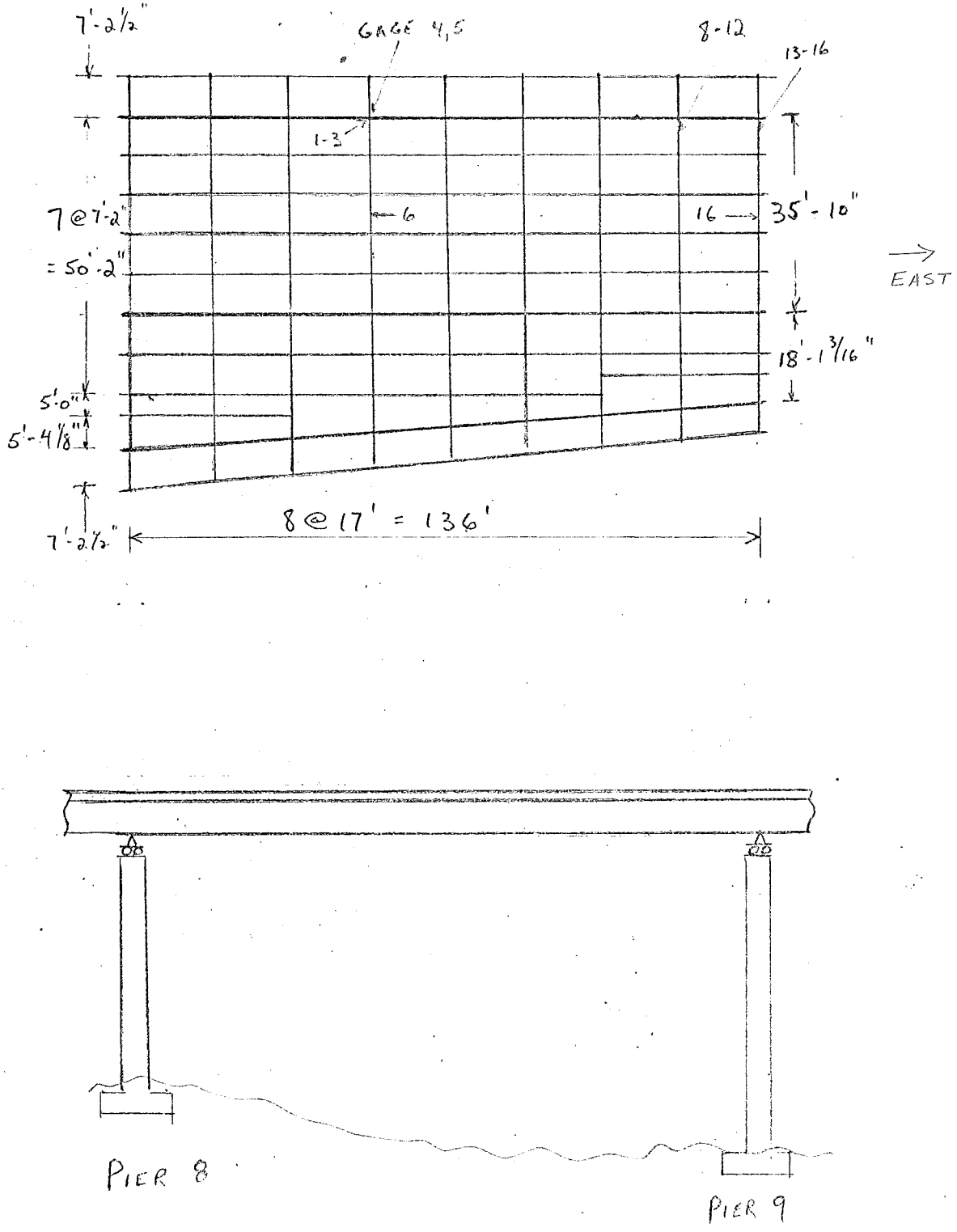

Fig. 4 Plan and Elevation of Interstate Route 81
Susquehanna River Bridge

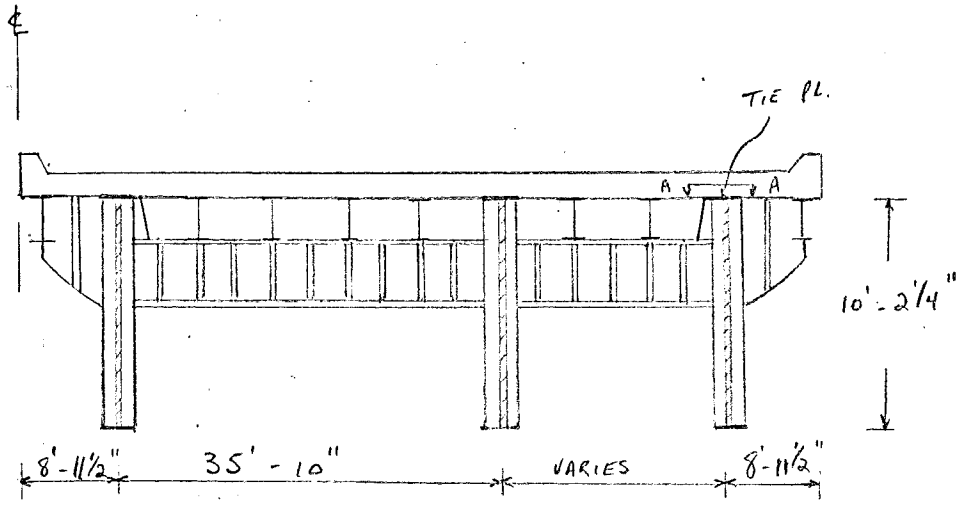

Fig. 5a Cross Section of Interstate Route 81 Susquehanna River Bridge

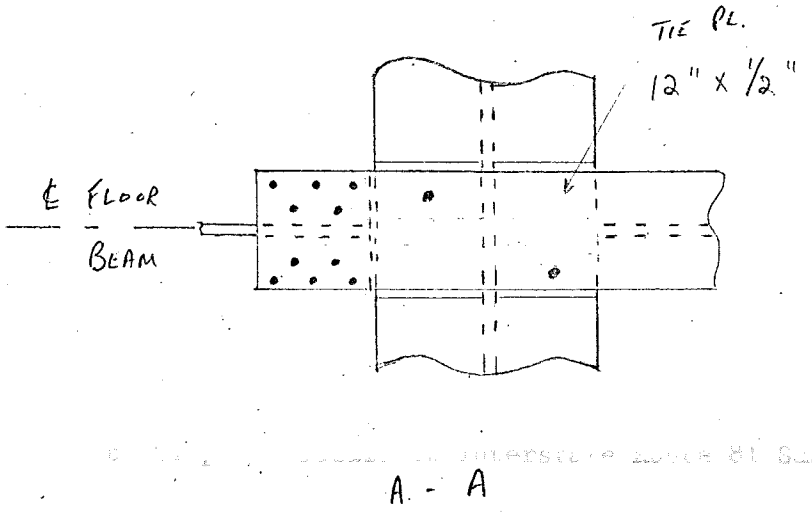

Fig. 5b Tieplate Detail at Interstate Route 81 Susquehanna River Bridge

Fig. 6 South Bridge

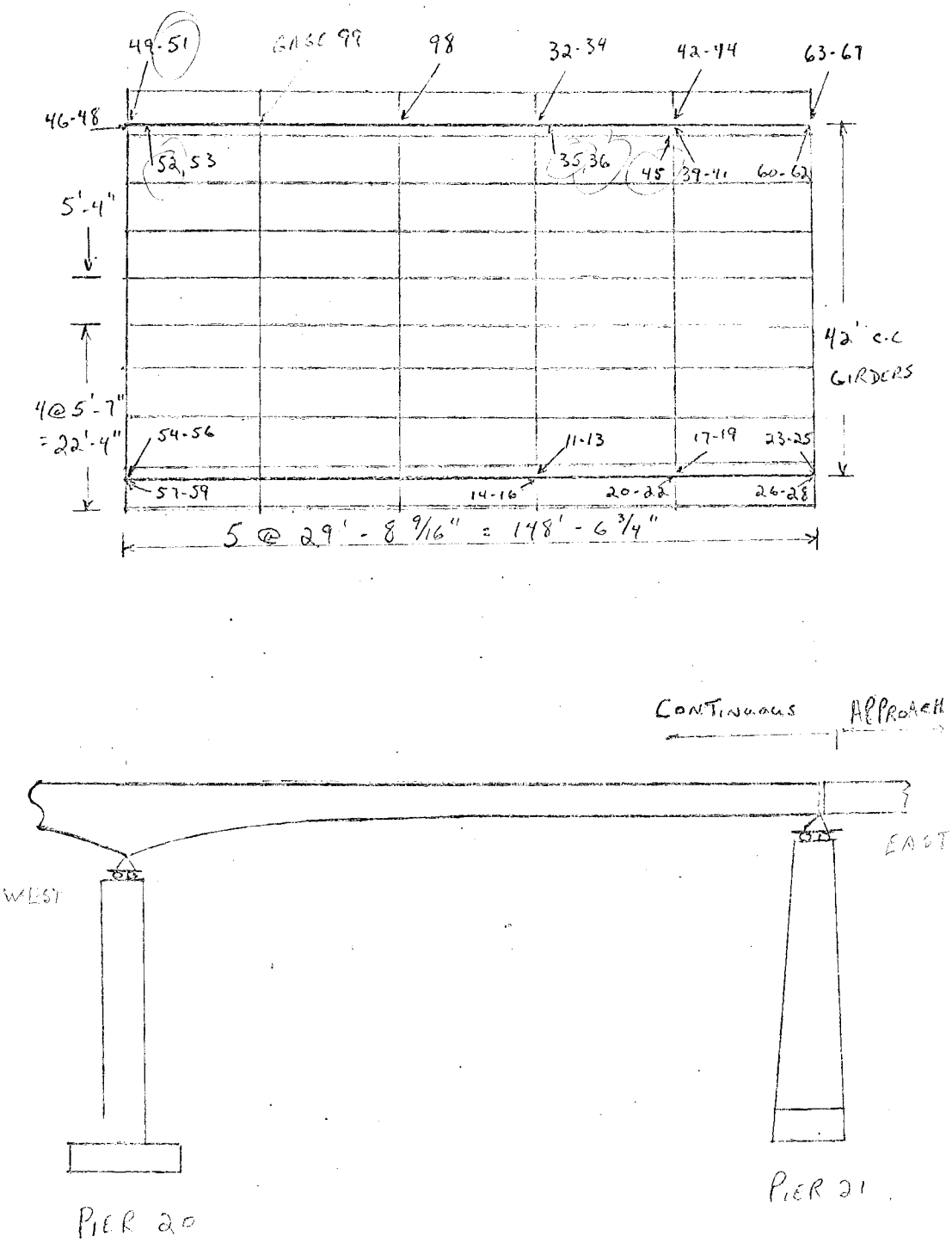

Fig. 7 Plan and Elevation of South Bridge

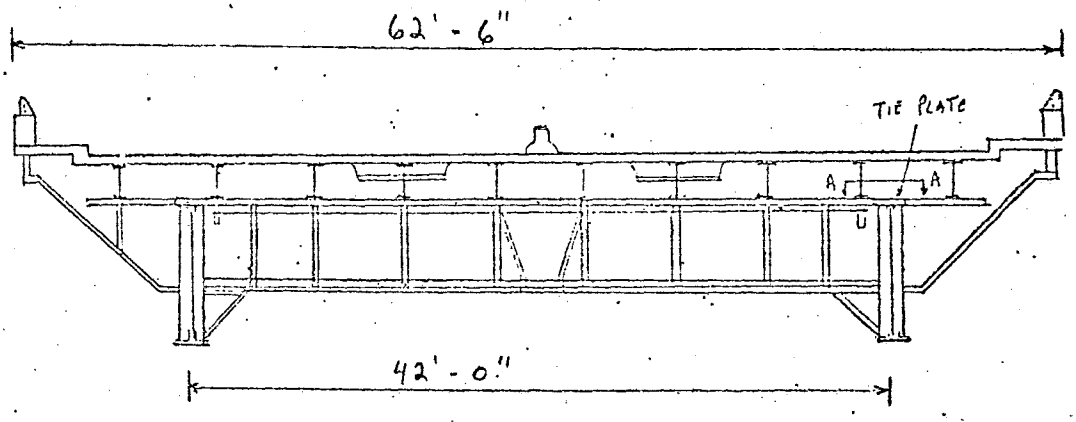

Fig. 8a Cross Section of South Bridge

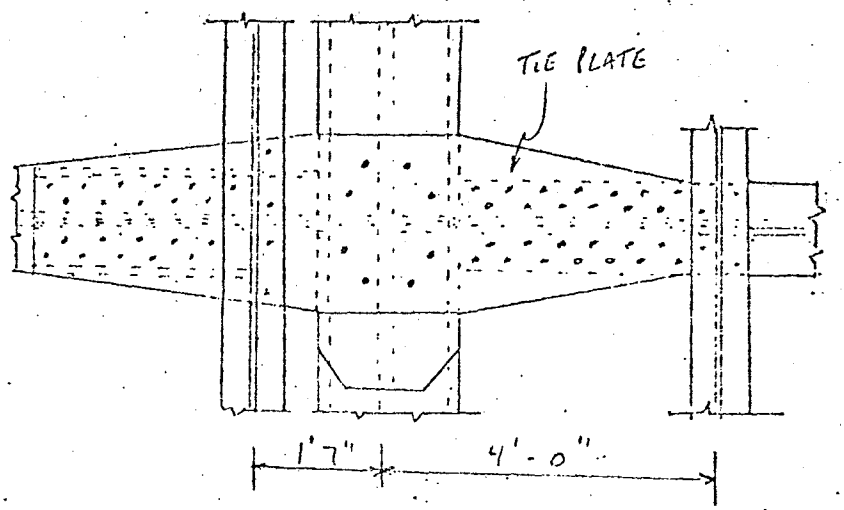

Fig. 8b Tieplate Detail at South Bridge

Fig. 9 West Chester Bridge

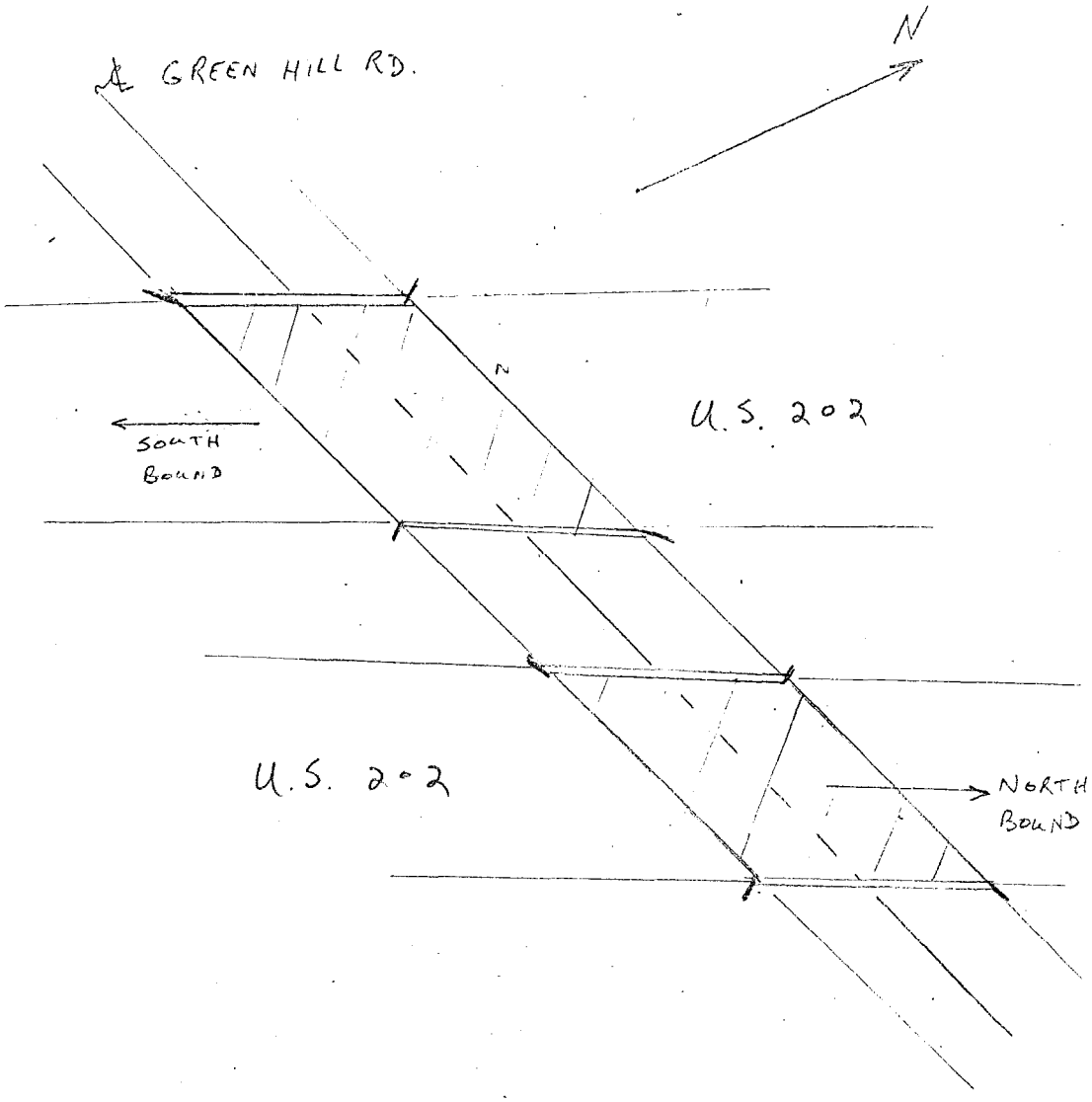

Fig. 10 Location of West Chester Bridge

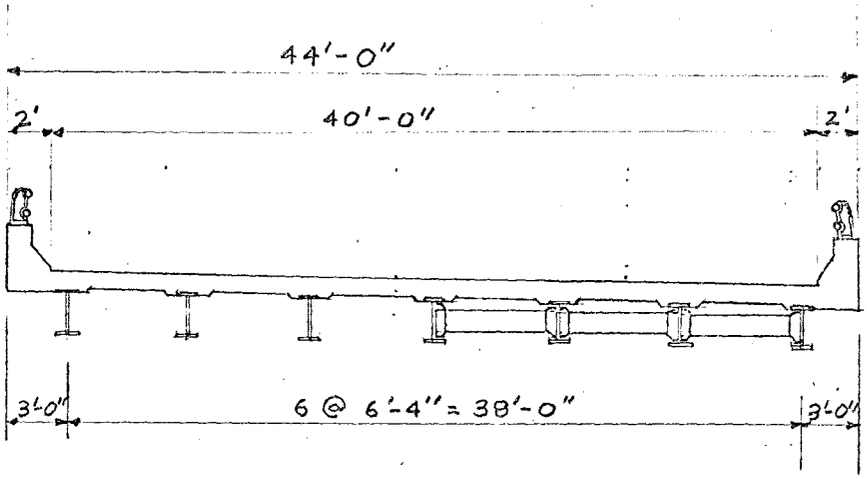

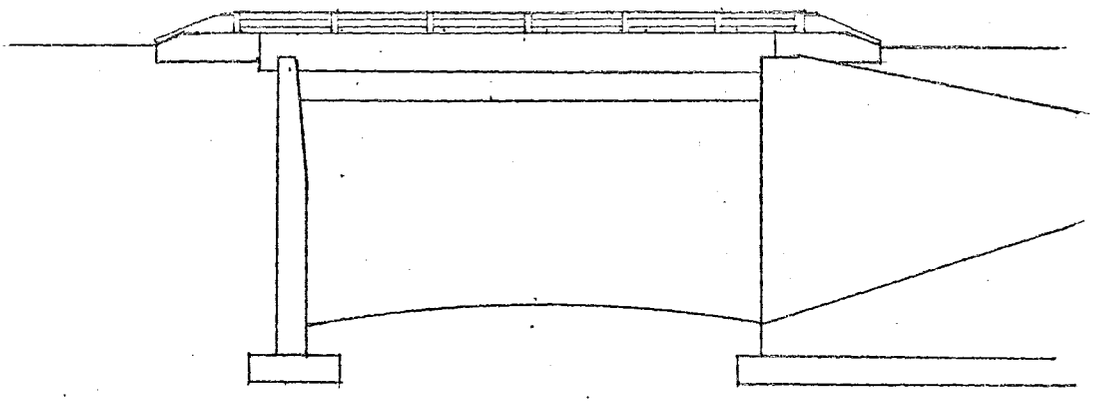

Fig. 11 Elevation and East View of West Chester Bridge

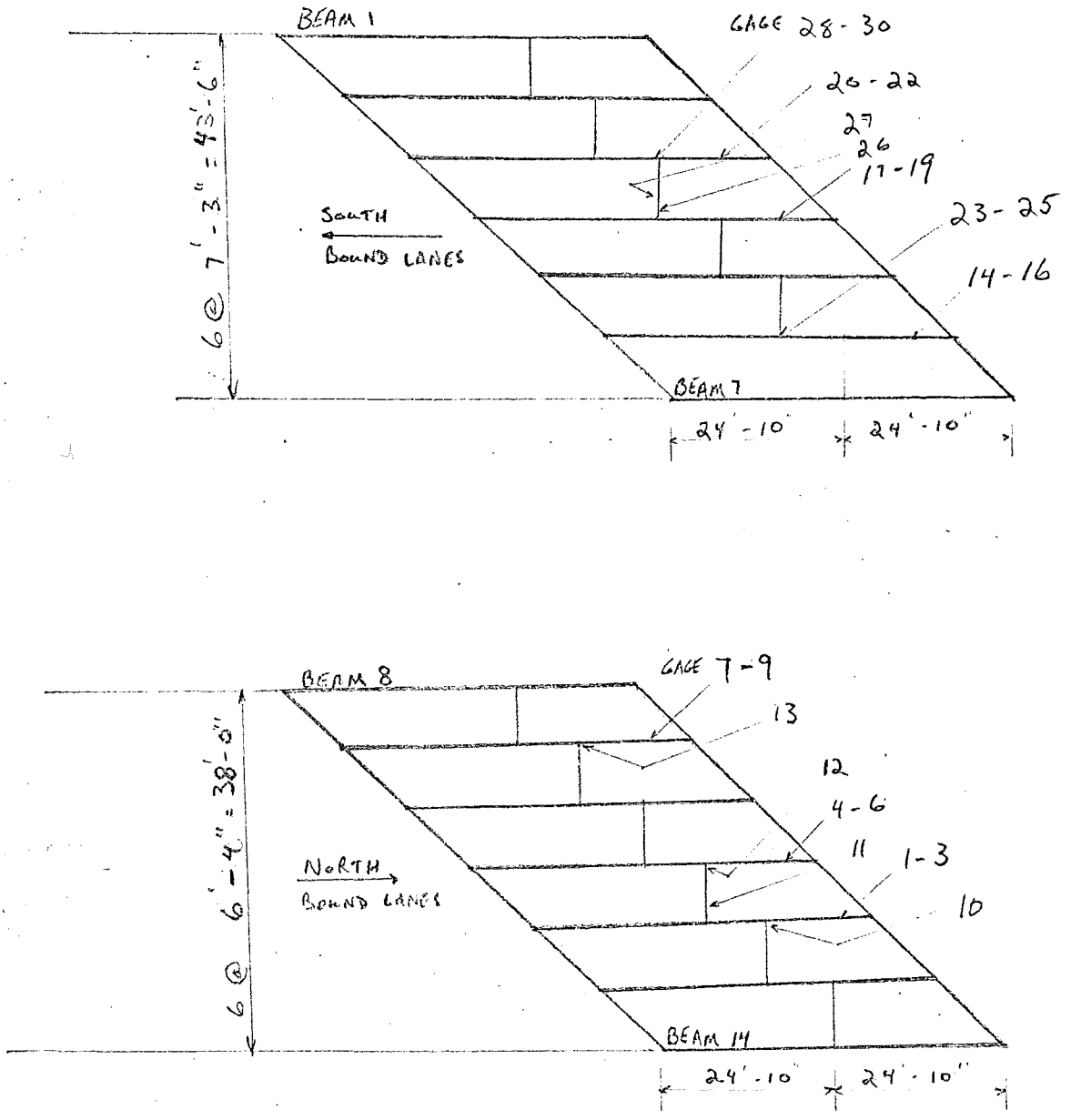

Fig. 12 Plan View of West Chester Bridge

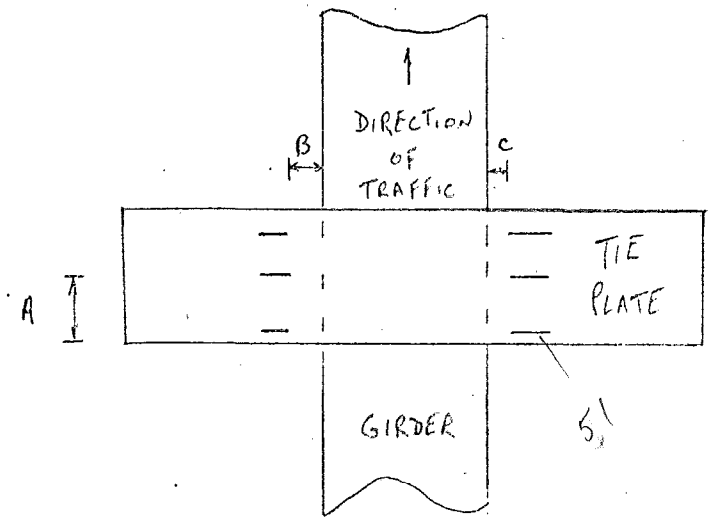

Fig. 13a Gages on Tieplate Details

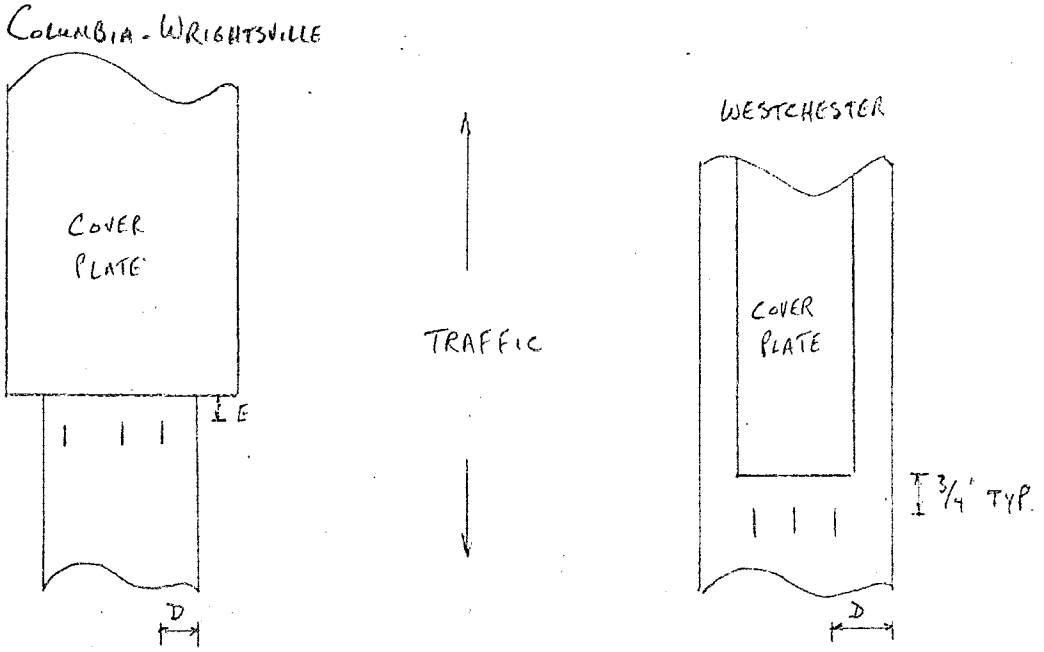

Fig. 13b Gages on Coverplated Beam

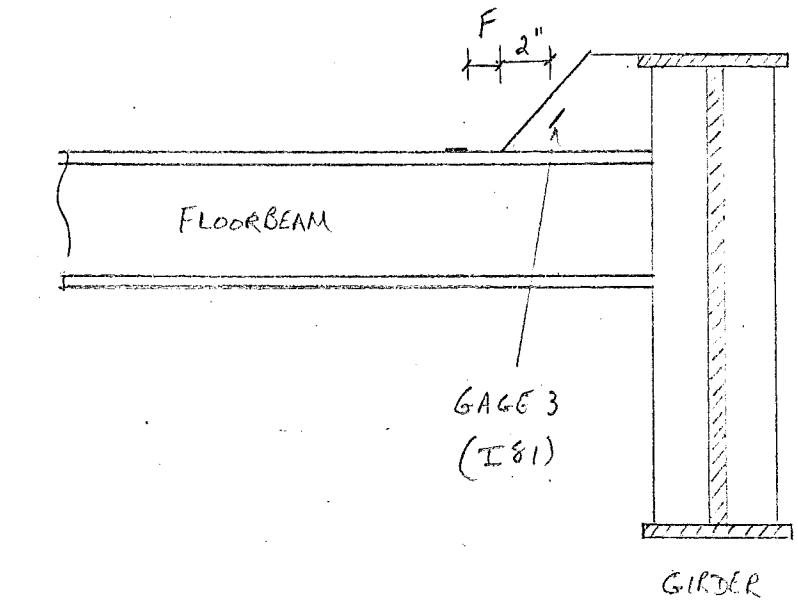

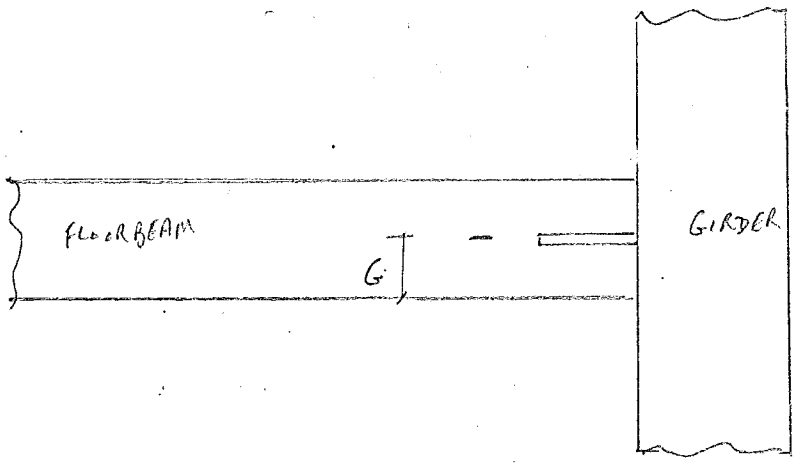

Fig. 14 Gages at Knee Brace Detail

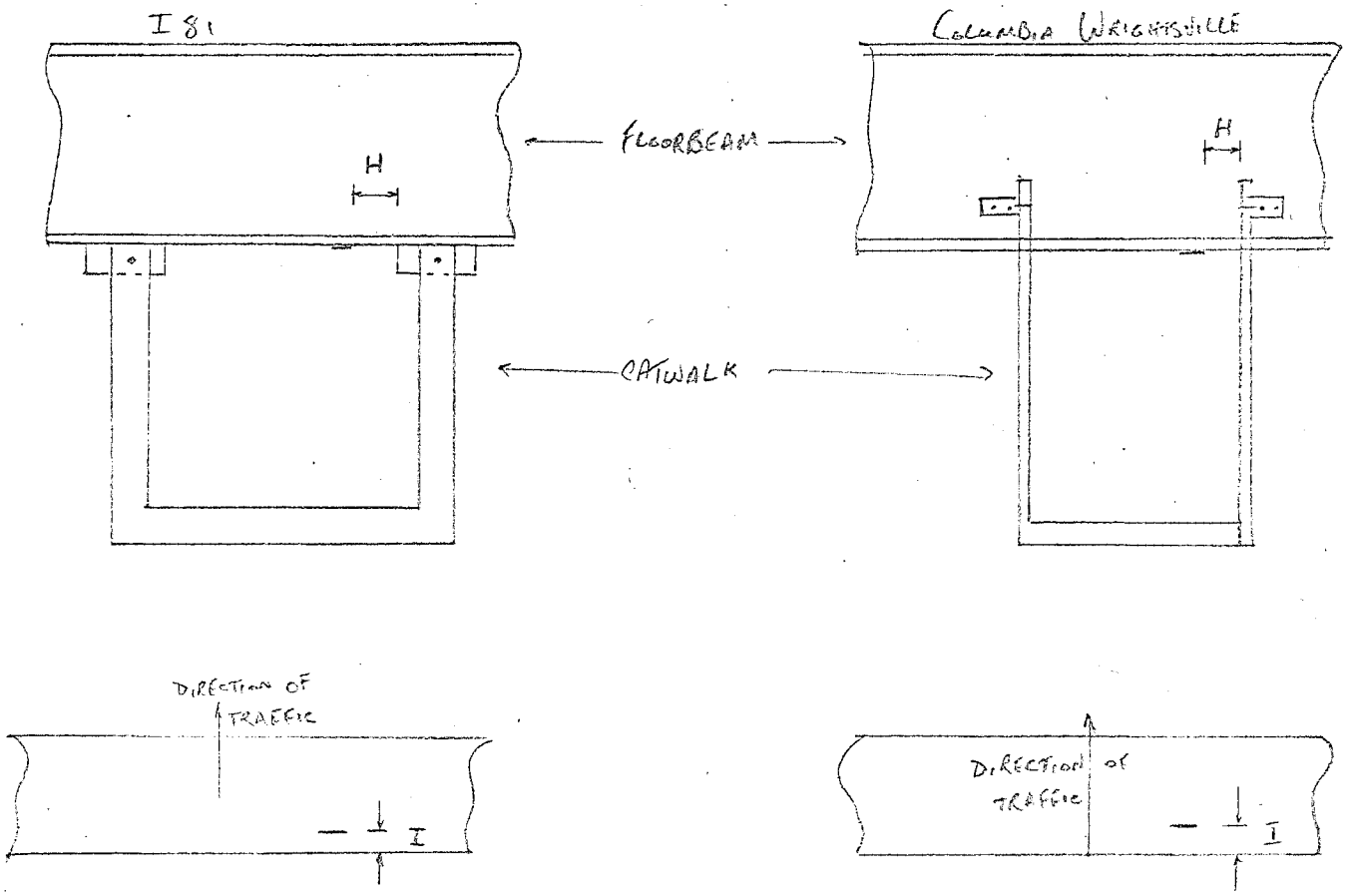

Fig. 15 Gages at Catwalk Attachment

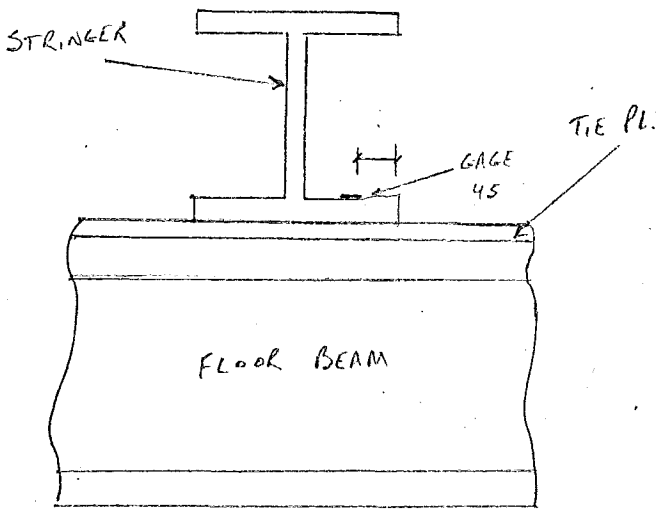

Fig. 16a Gages on South Bridge Stringer

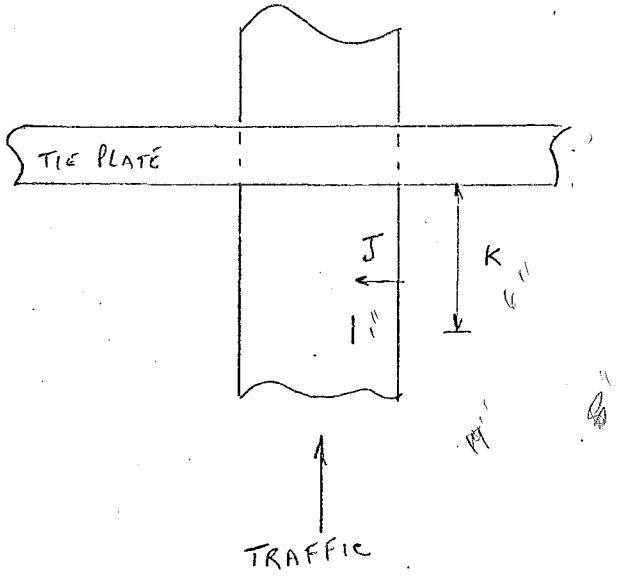

Fig. 16b Gages on South Bridge Girder

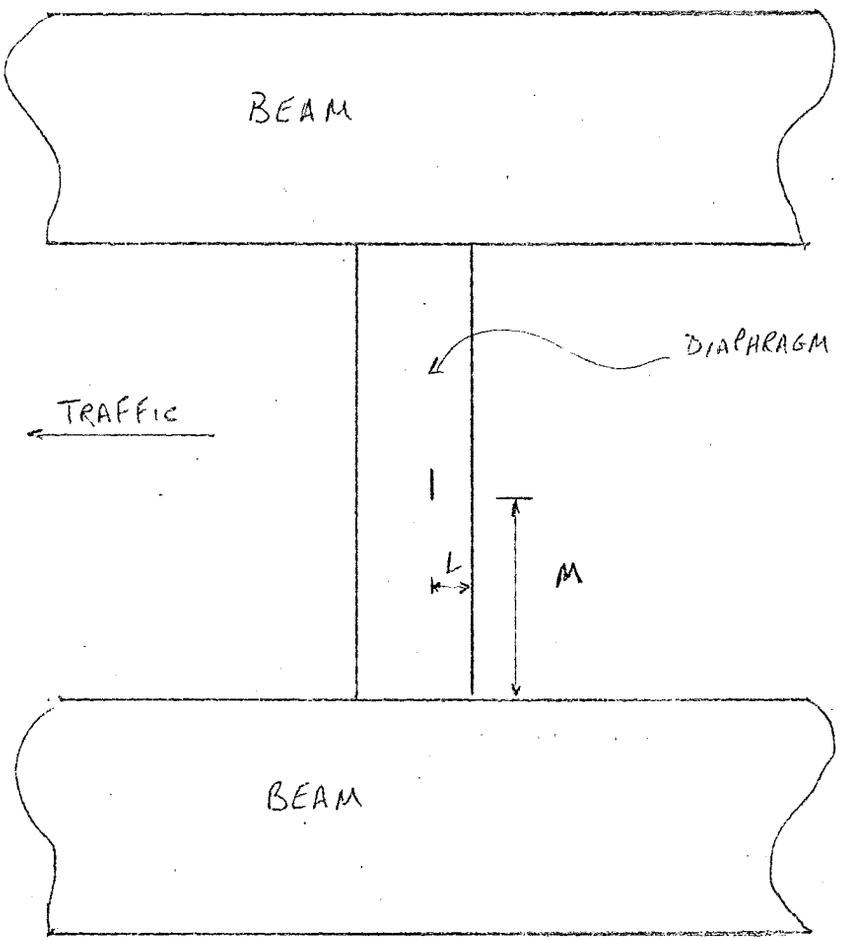

Fig. 17 Gages on Diaphragm

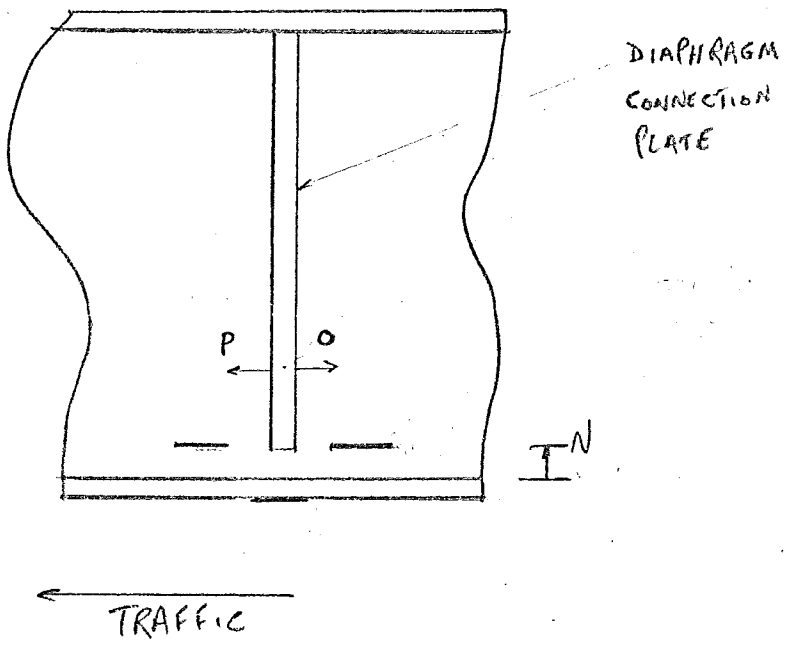

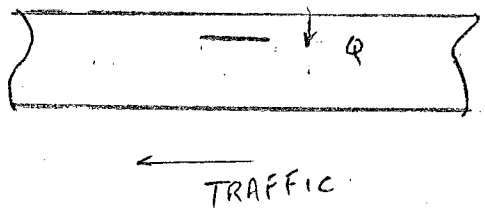

Fig. 18 Gages at Diaphragm to Beam Connection

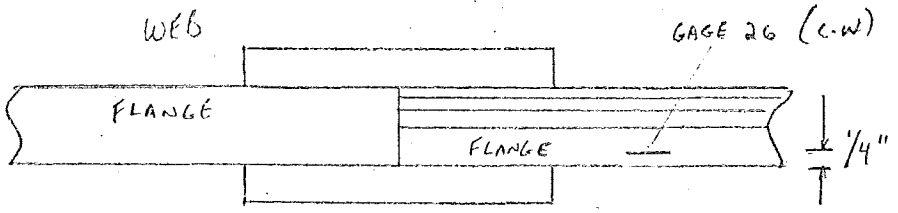

Fig. 19a Gage at Columbia-Wrightsville Bridge Girder Splice

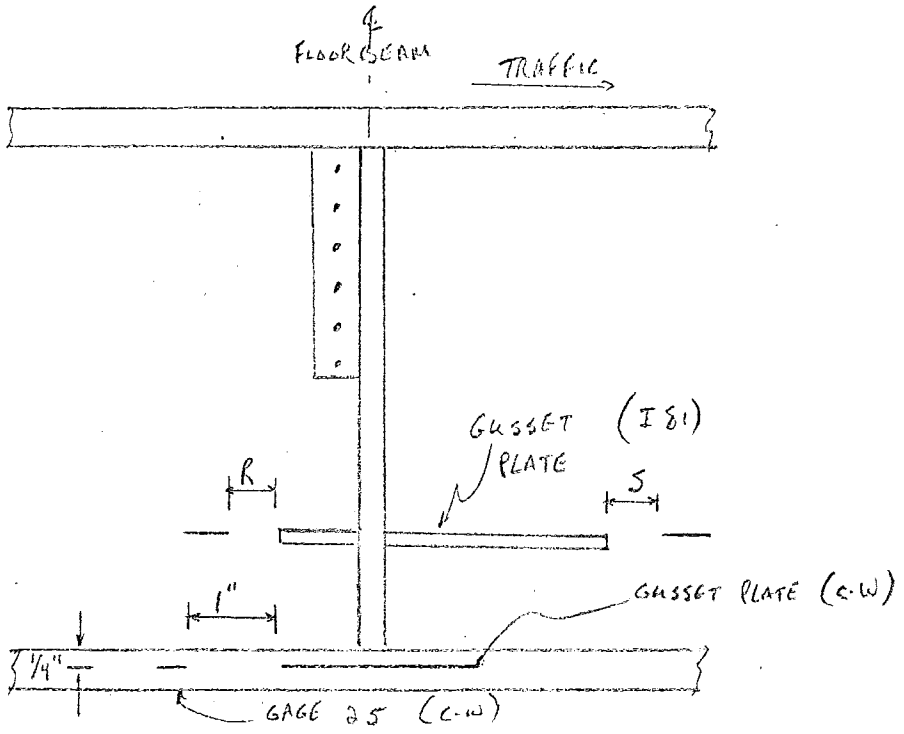

Fig. 19b Gages on Gusset Plate Detail

TYPE	CODE
BUS	B
2-AXLE TRUCK 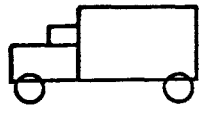	2D
3-AXLE TRUCK 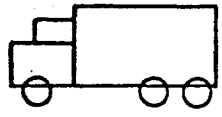	3
3-AXLE TRACTOR SEMI-TRAILER 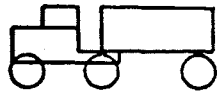	2S-1
4-AXLE TRUCK 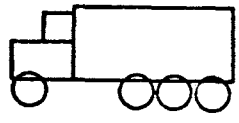	4
4-AXLE TRACTOR SEMI-TRAILER 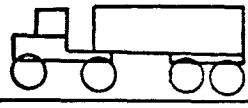	2S-2
5-AXLE TRACTOR SEMI-TRAILER 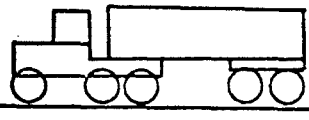	3S-2

Fig. 20 Truck Classification (FHWA)

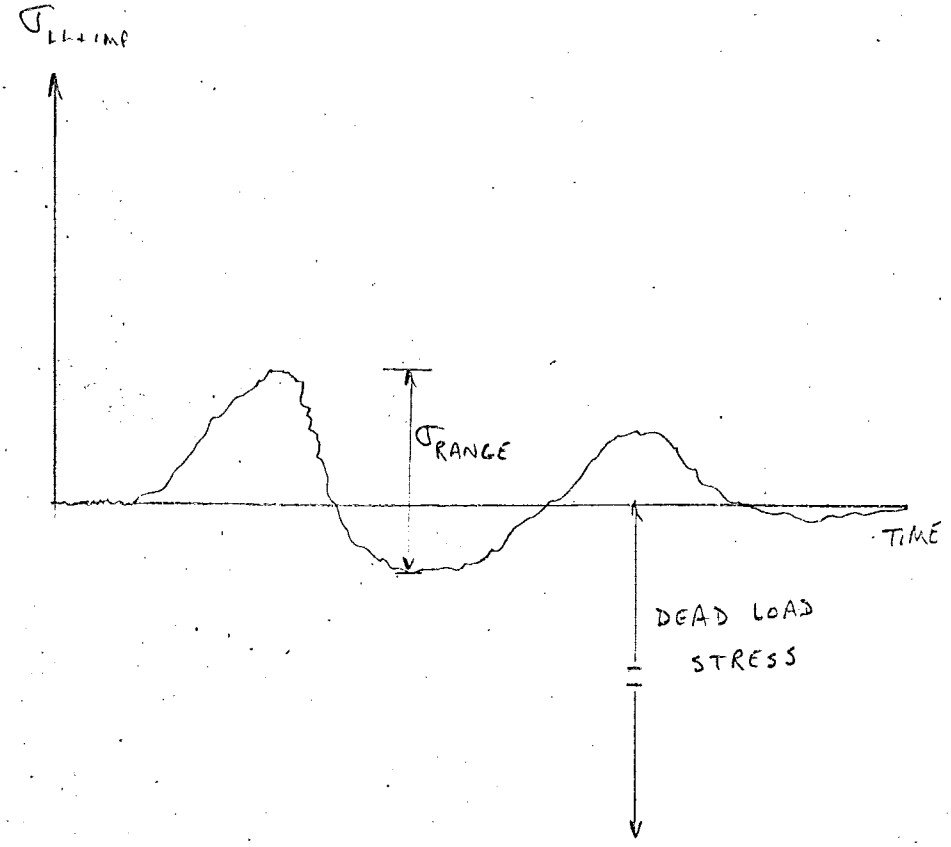

Fig. 21 Typical Analog Measurement of Live Load Stresses

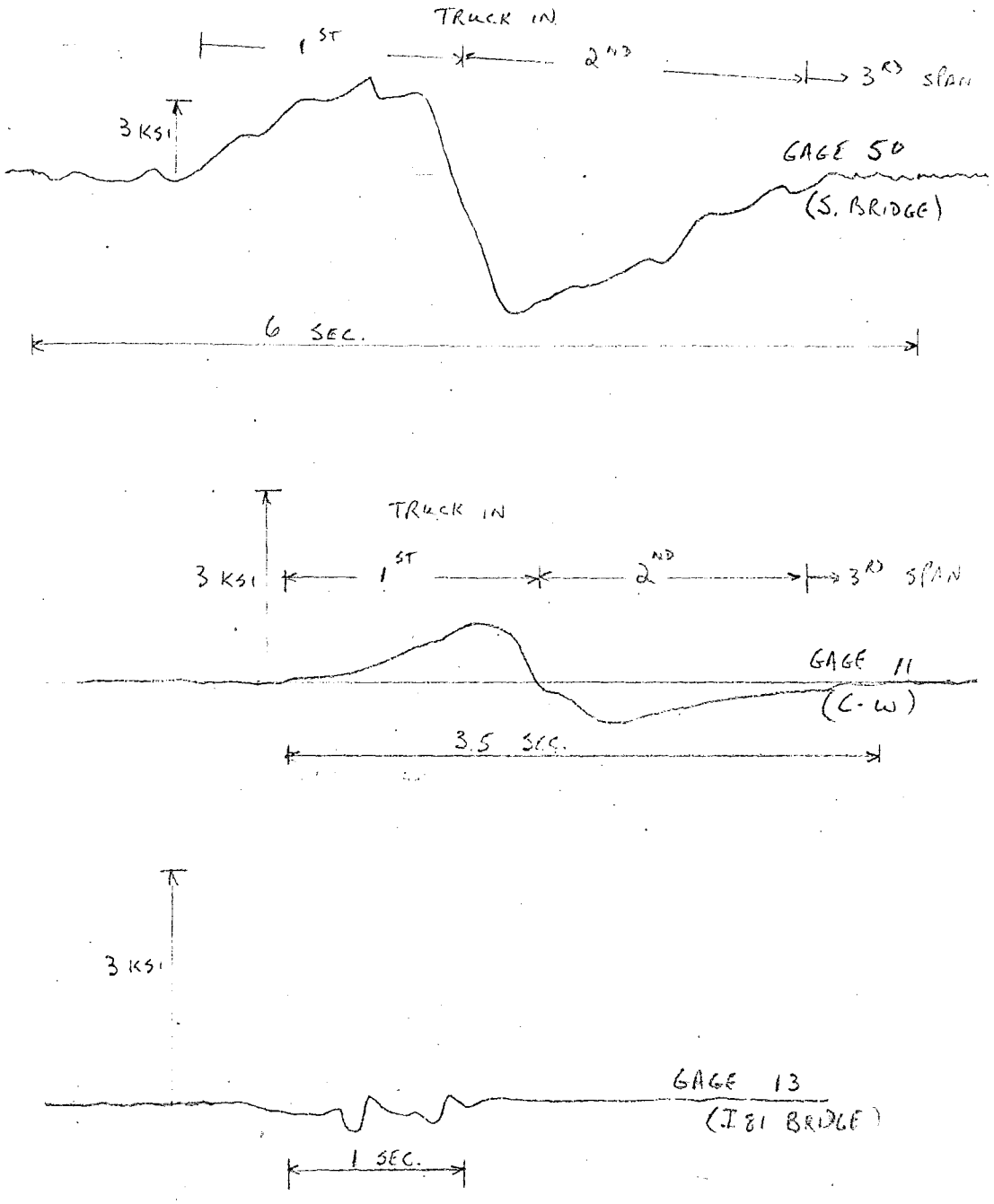

Fig. 22 Comparison of Tieplate Strain Histories

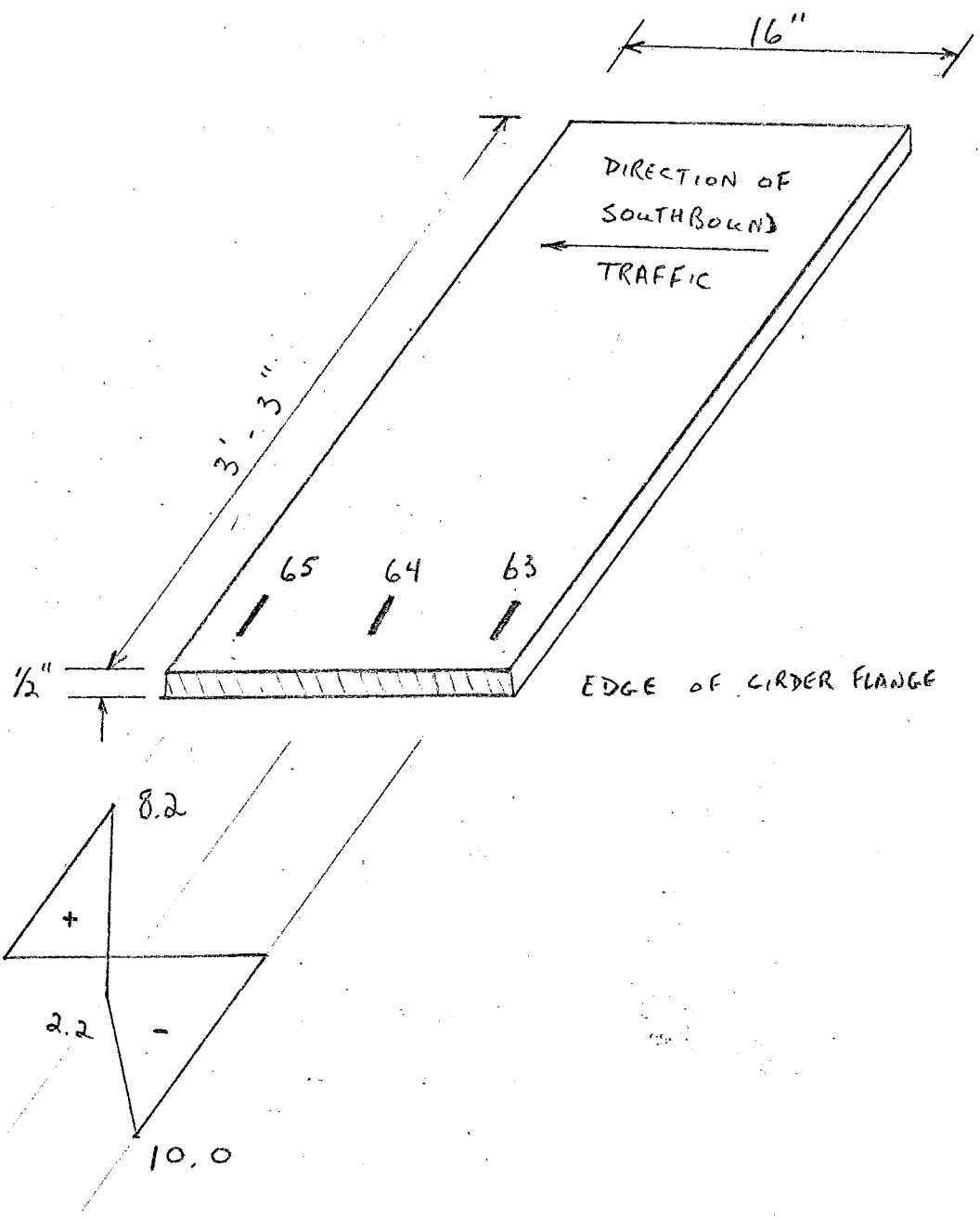

Fig. 23 Instantaneous Stress Distribution in South Bridge Tieplate

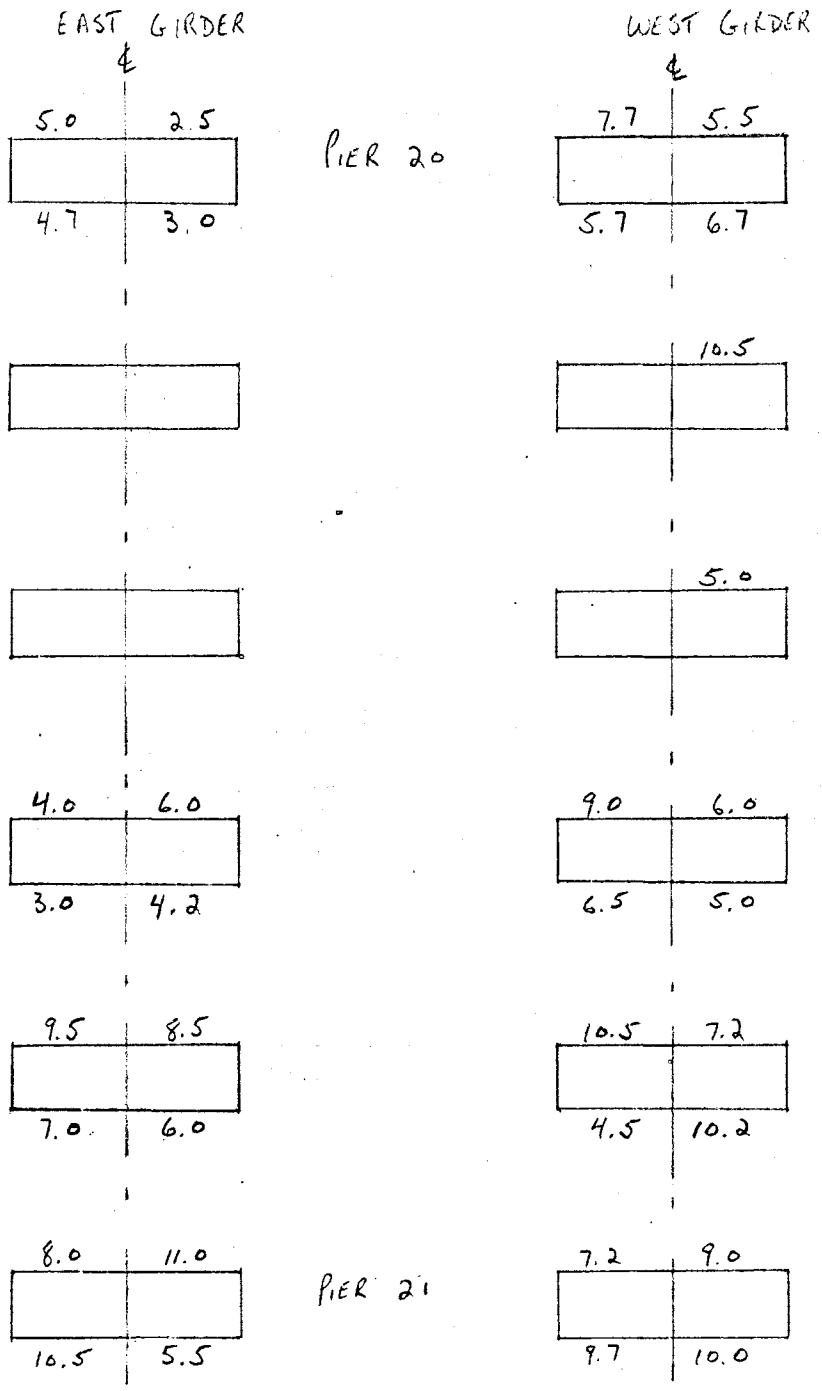

Fig. 24 Maximum Recorded South Bridge Tieplate Stresses

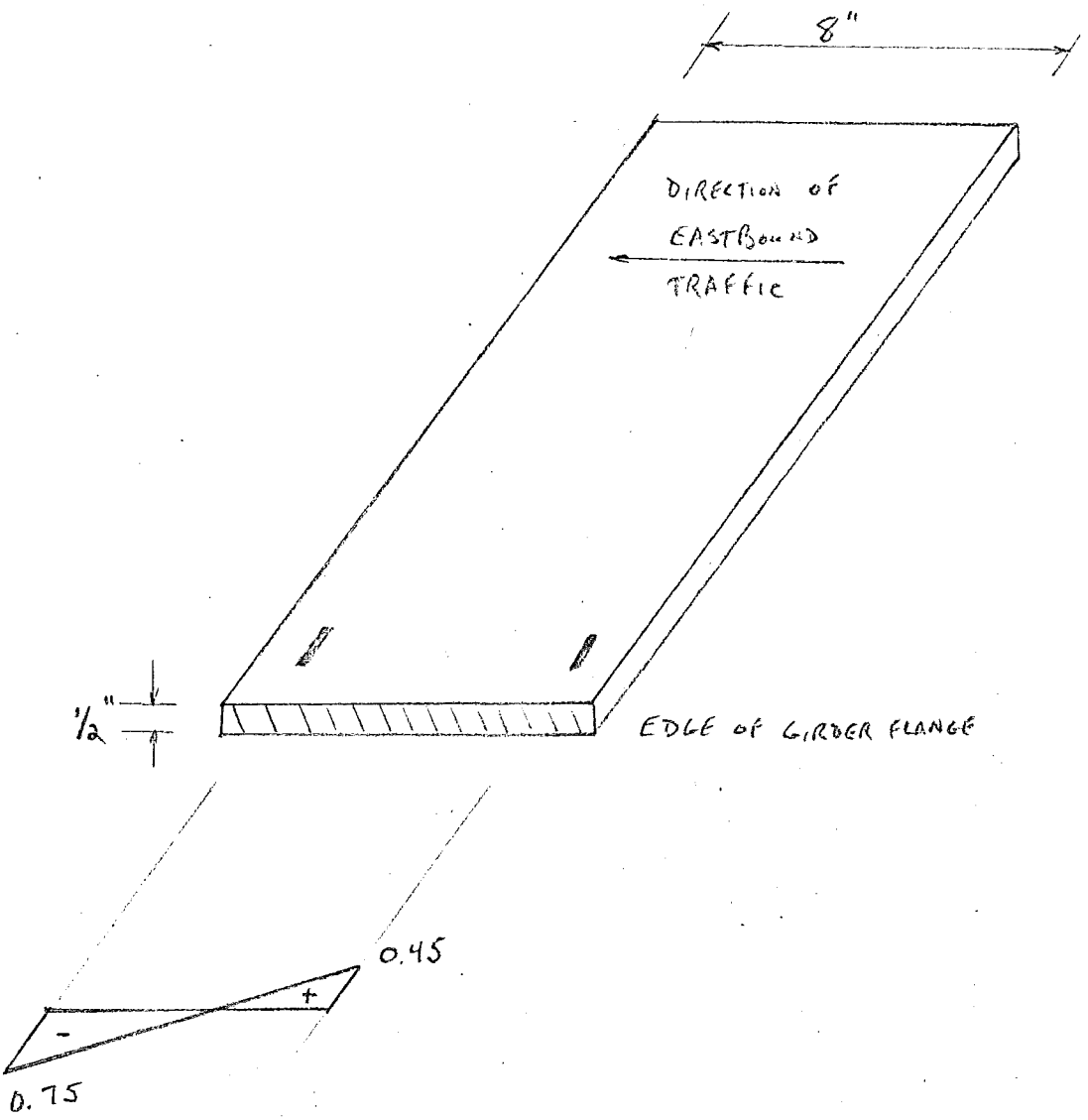

Fig. 25 Instantaneous Stress Distribution in Columbia-Wrightsville Bridge Tieplate

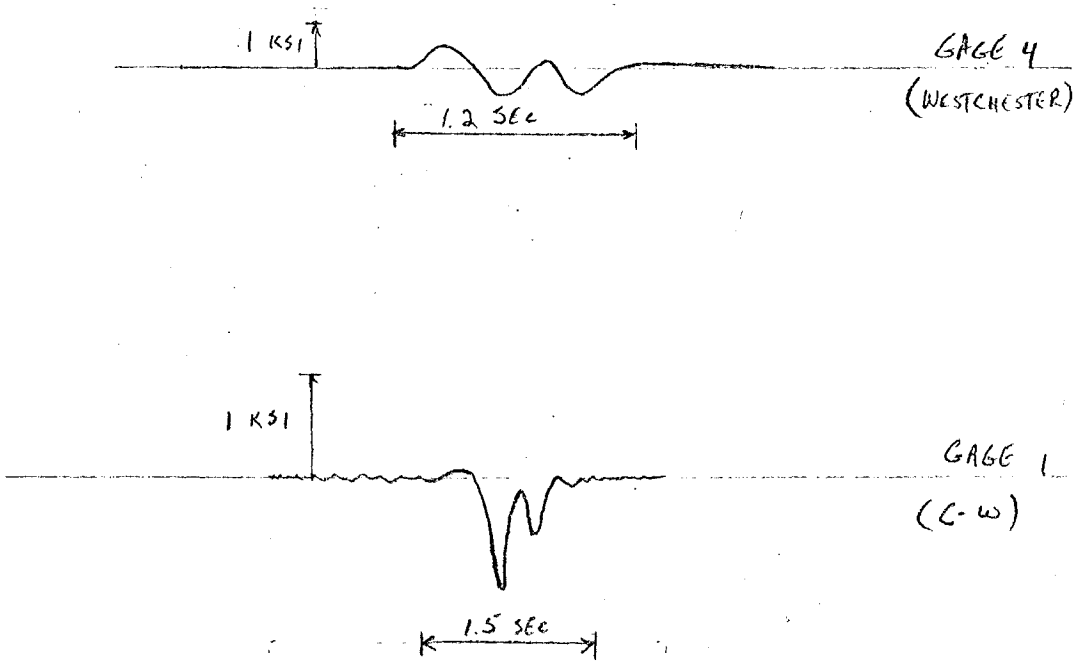

Fig. 26 Comparison of Coverplated Beam Strain Histories

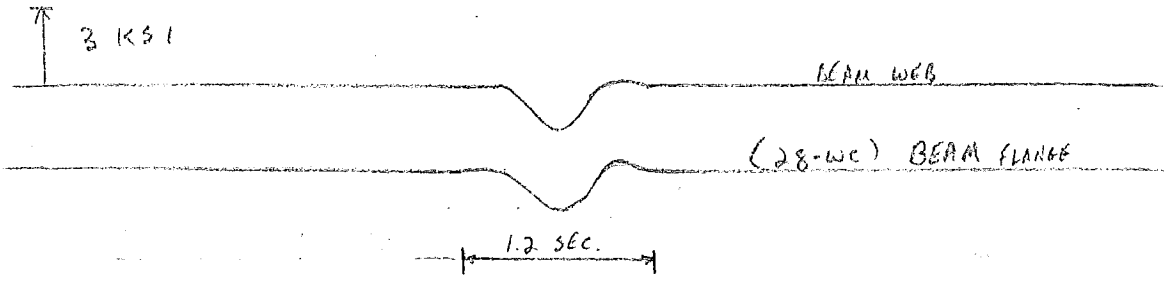

Fig. 27a Comparison of Strain Histories for Gages near Diaphragm Connection

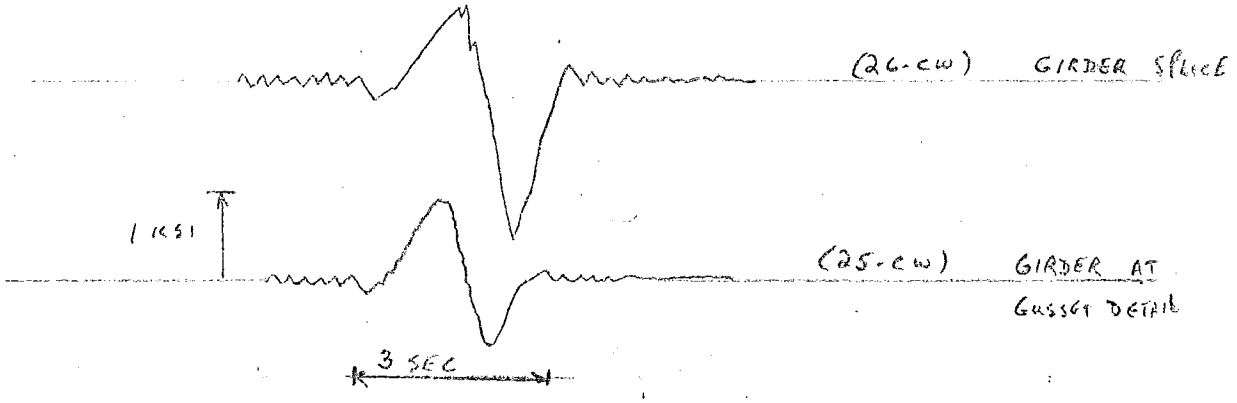

Fig. 27b Comparison of Strain Histories for Gages on Columbia-Wrightsville Bridge Girder

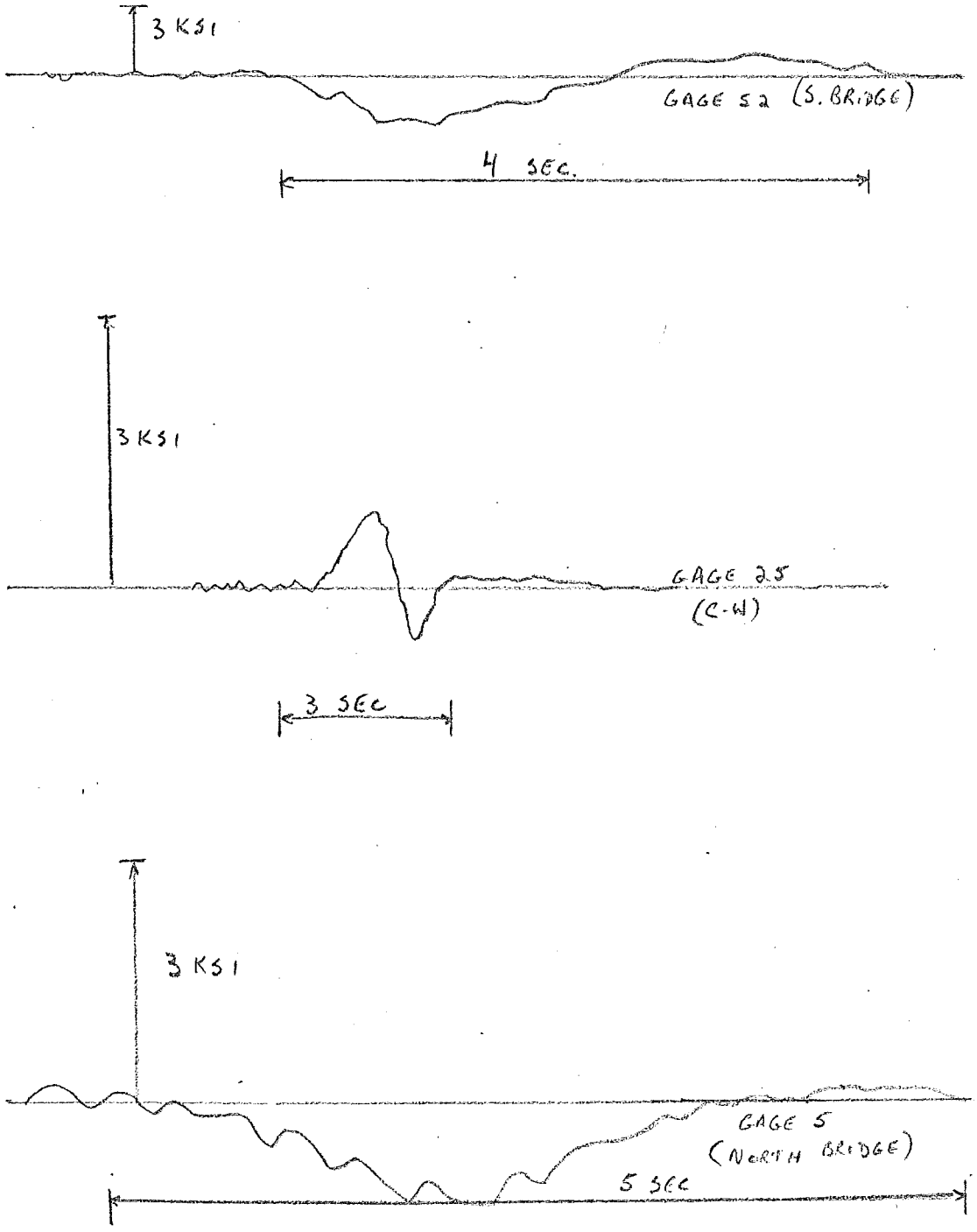

Fig. 28 Comparison of Girder Strain Histories

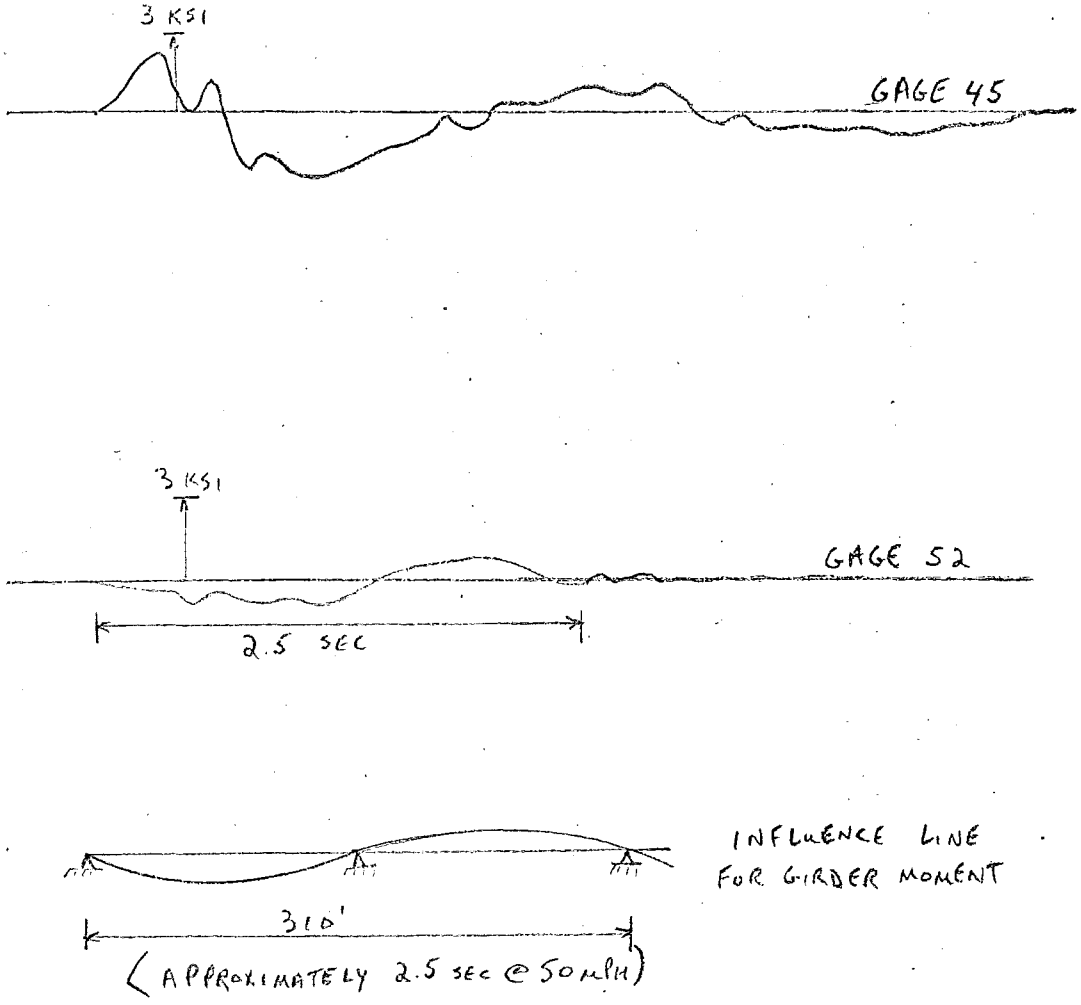

Fig. 29 Comparison of Girder and Stringer Strain Histories with Influence Line for Girder Moment

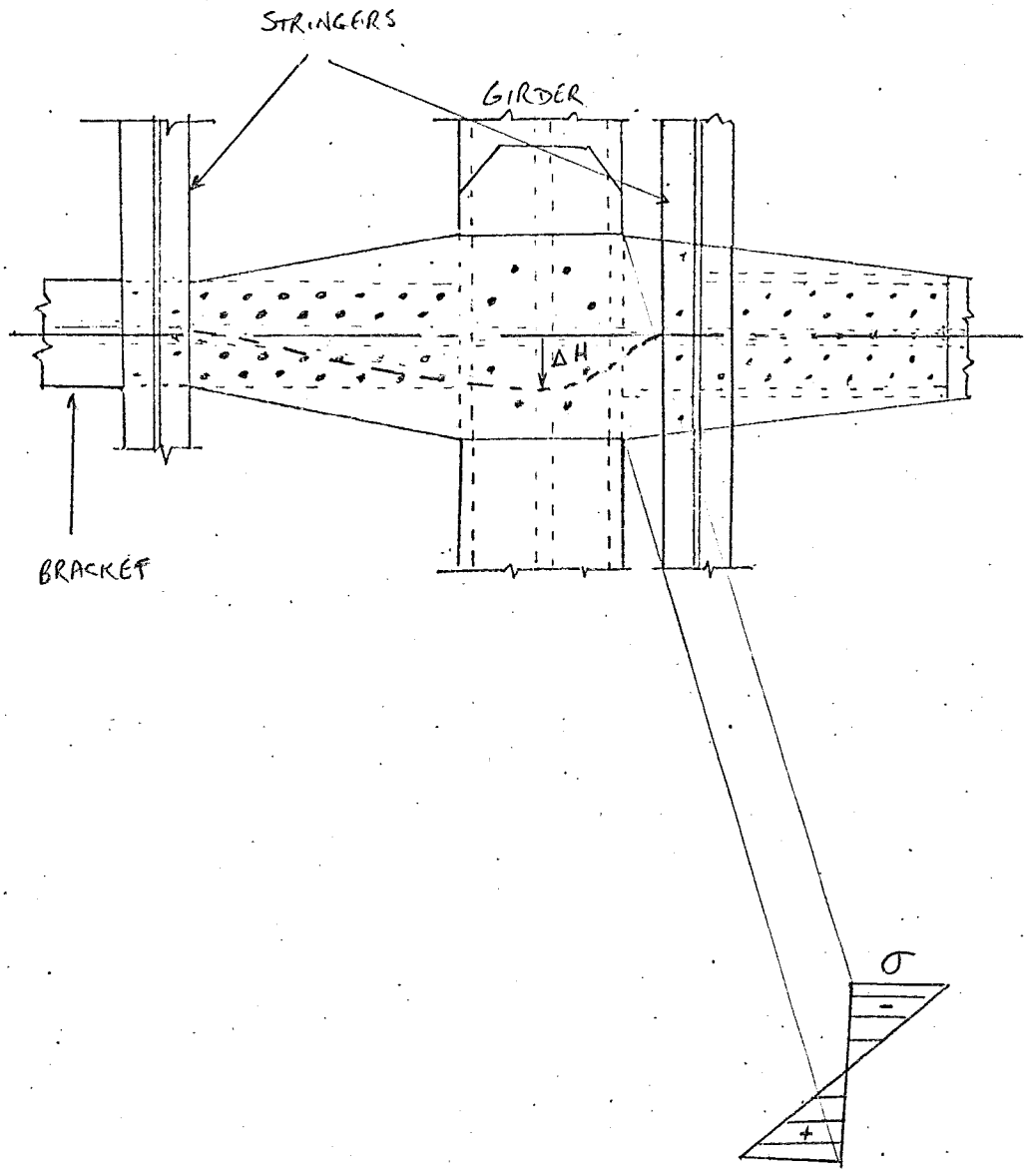

Fig. 30 Horizontal Displacement of Tieplate

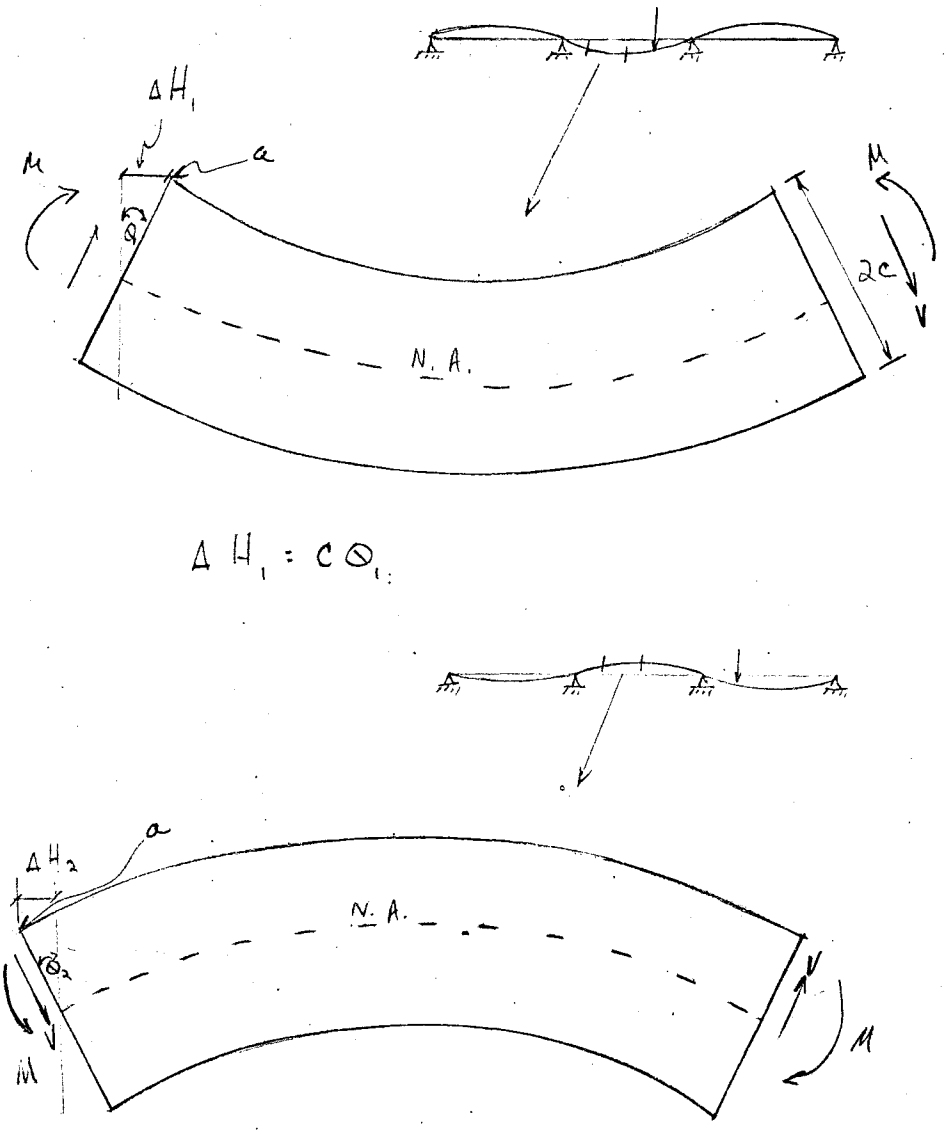

Fig. 31 Horizontal Displacement of a Point on the Girder Flange

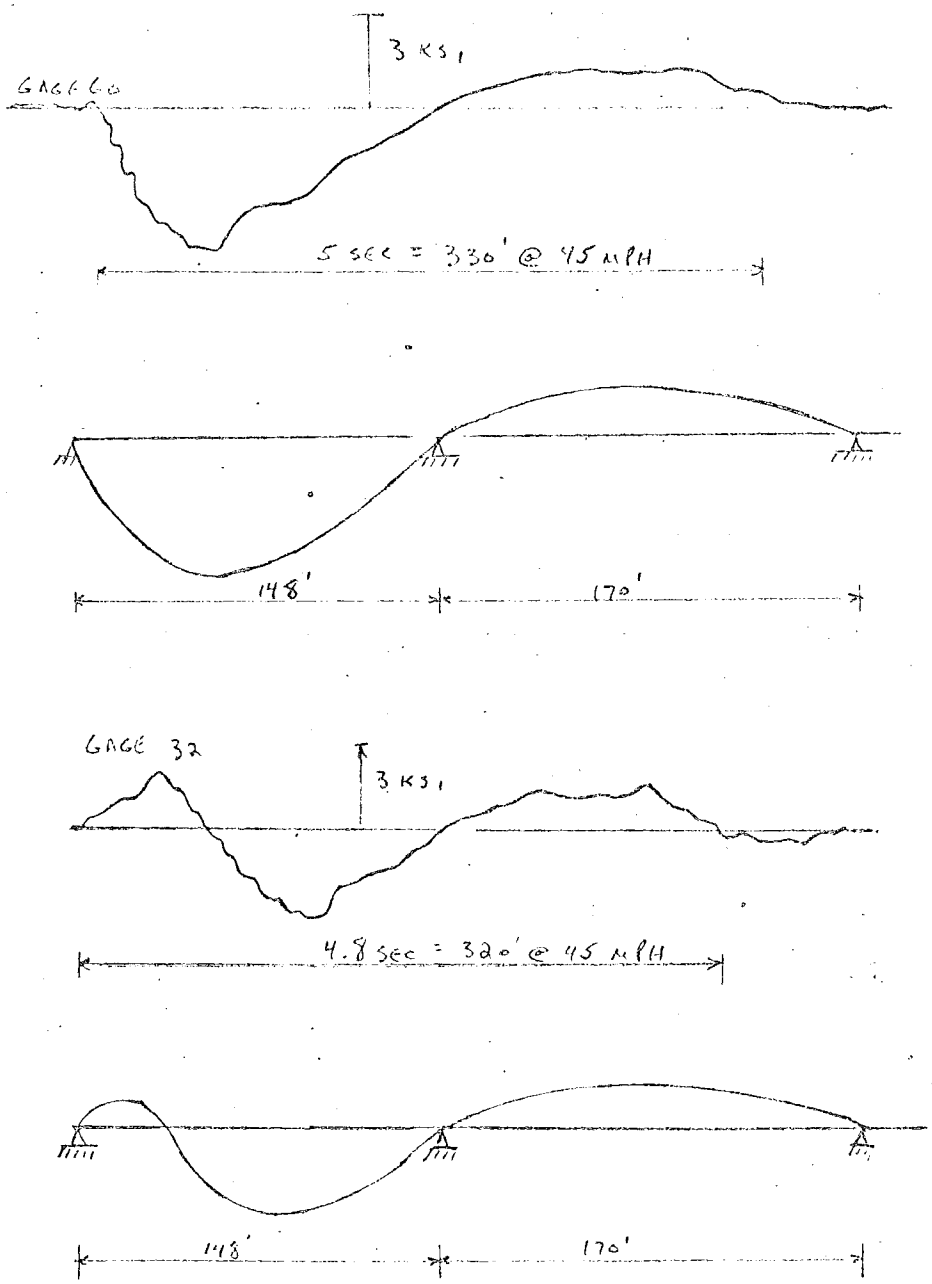

Fig. 32 Comparison of Tieplate Strain Histories with Influence Lines for Girder Slope

(SOUTH BRIDGE)

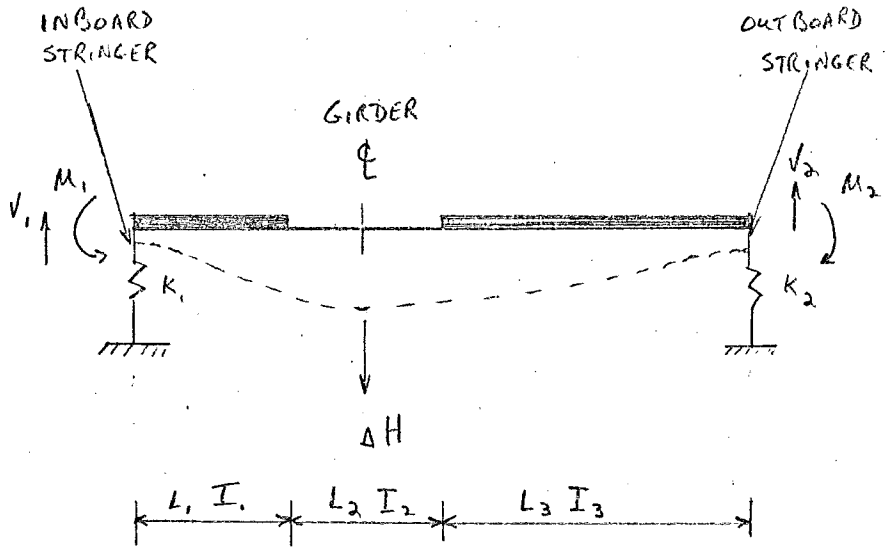

Fig. 33 Analytical Model for Tieplate

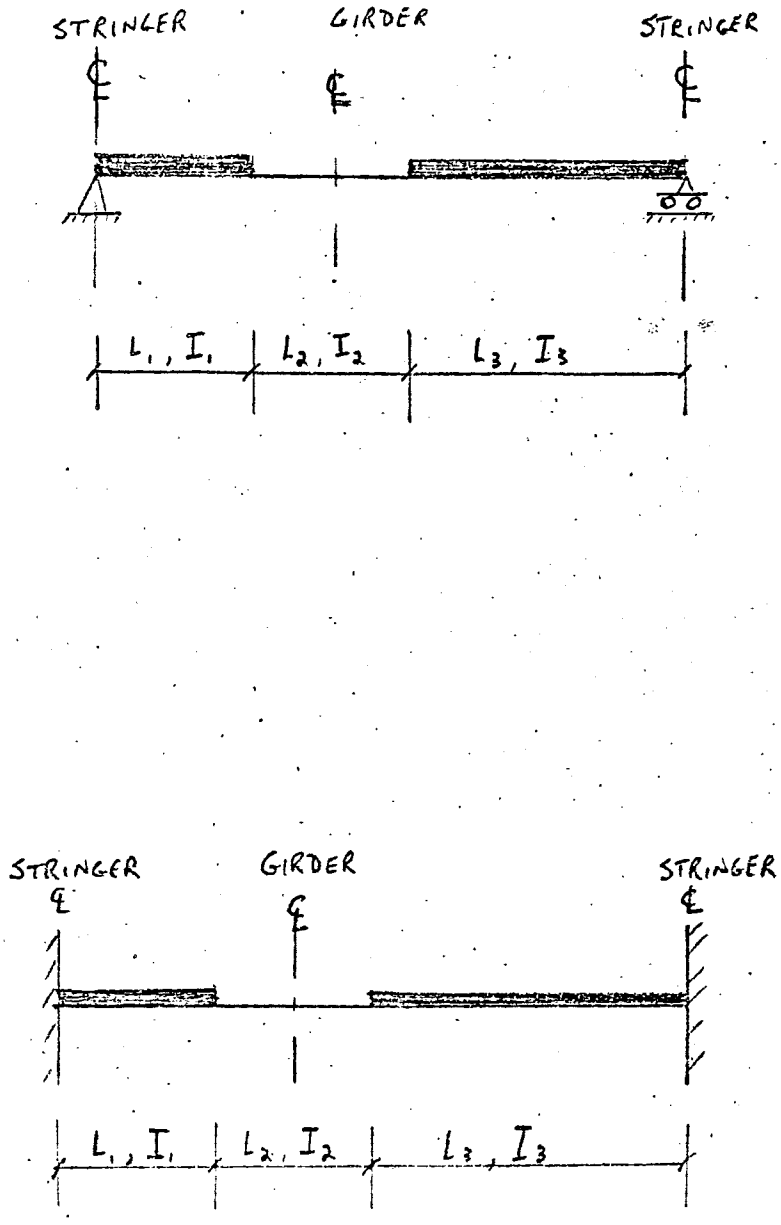

Fig. 34 Boundary Conditions for Analytical Model

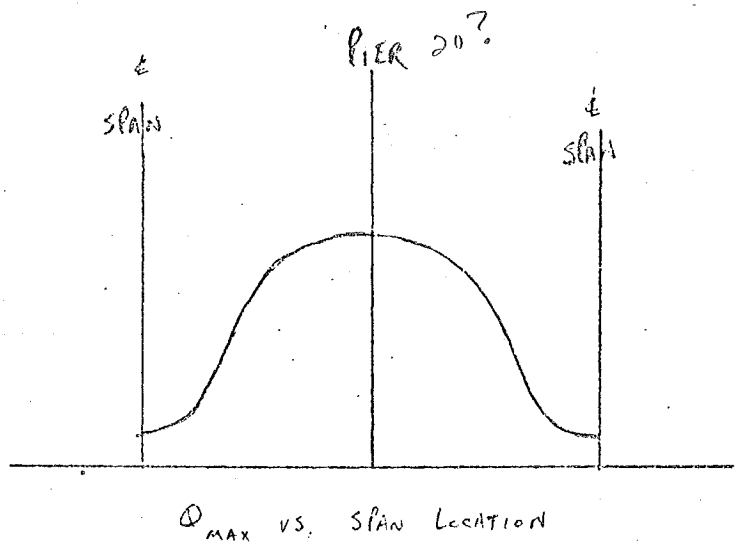

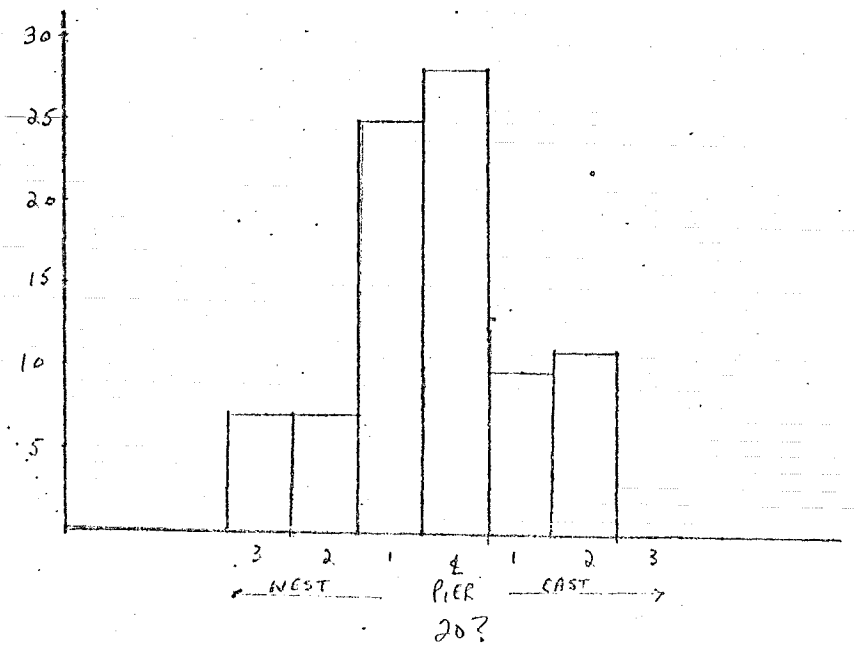

Fig. 35 Comparison of Location of South Bridge River Failures with Envelope for Girder Slope

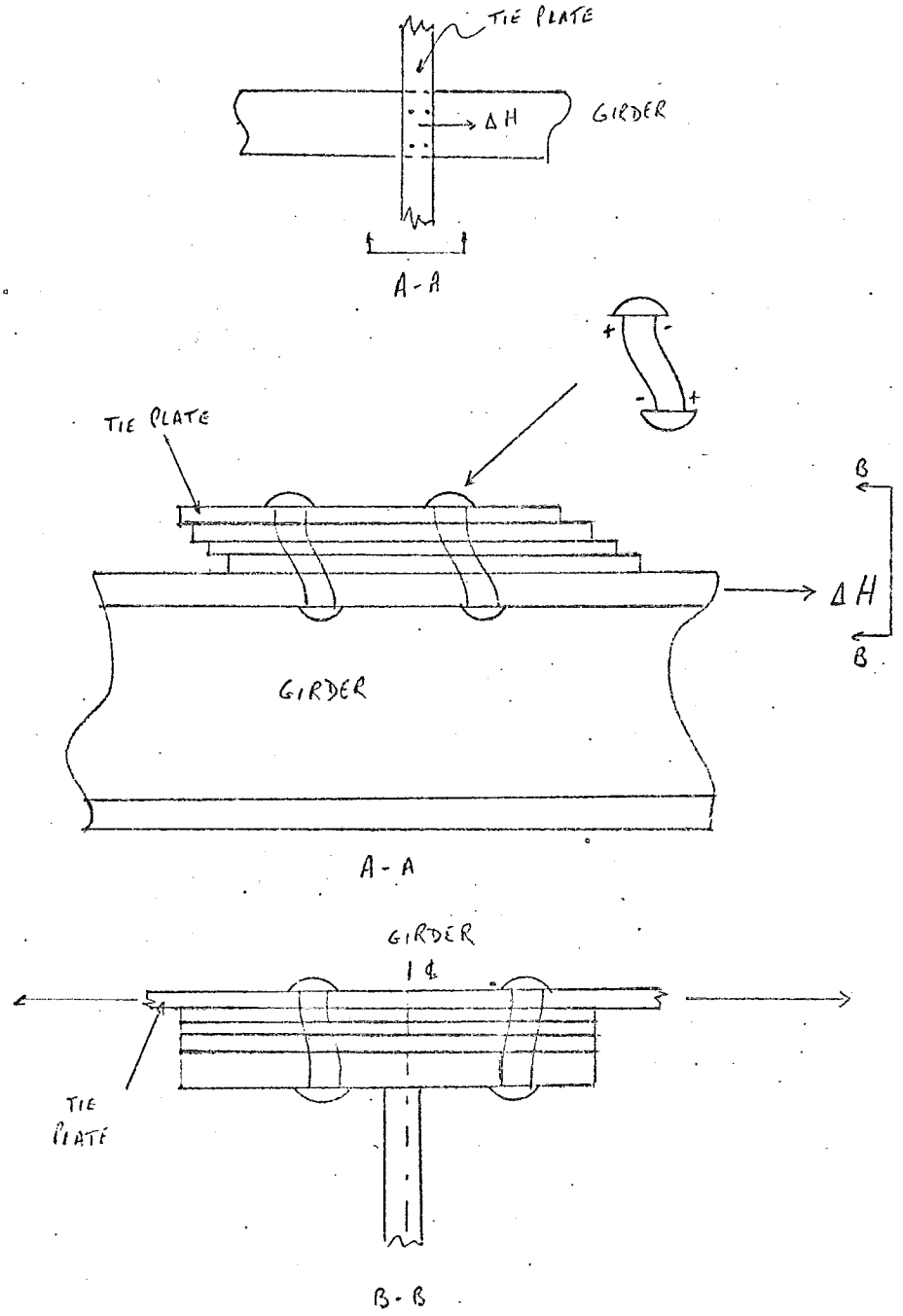

Fig. 36 Differential Displacement of Tieplate in Longitudinal and Lateral Directions

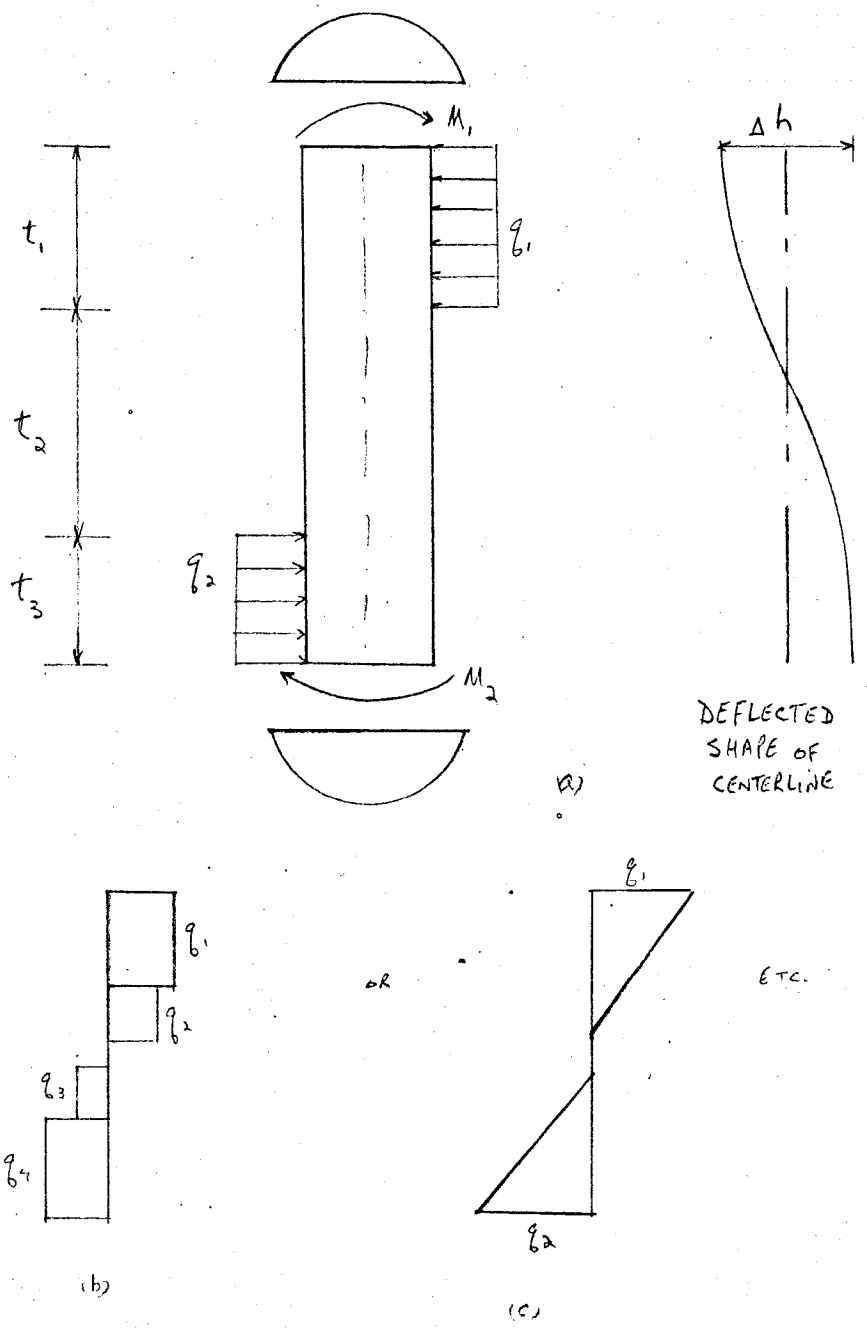

Fig. 37 Rivet as Beam Element with Possible Bearing Stress Distributions

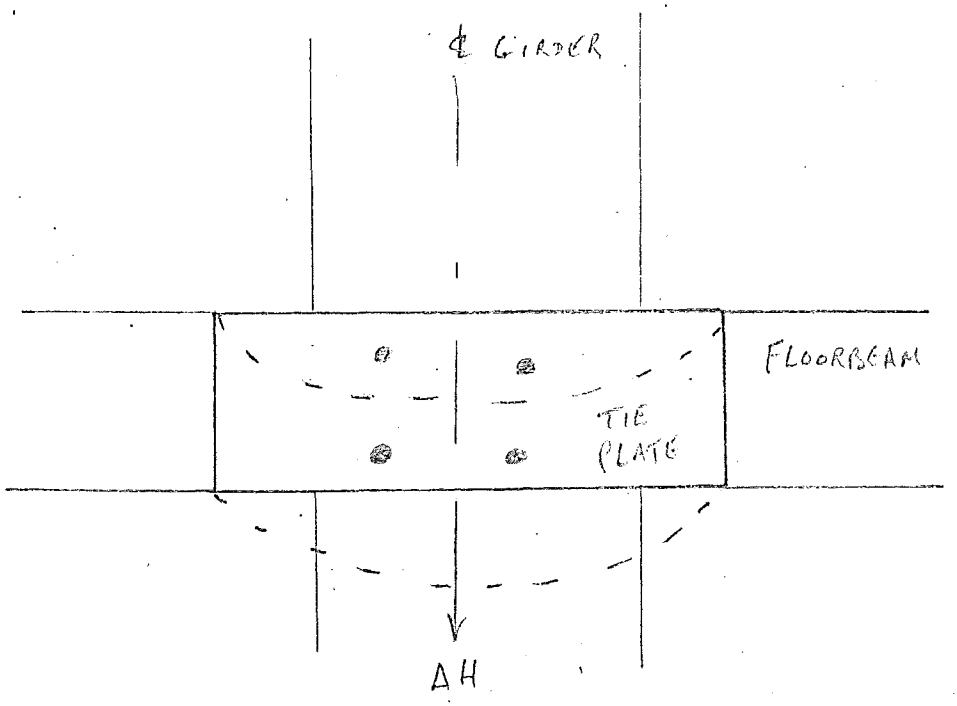

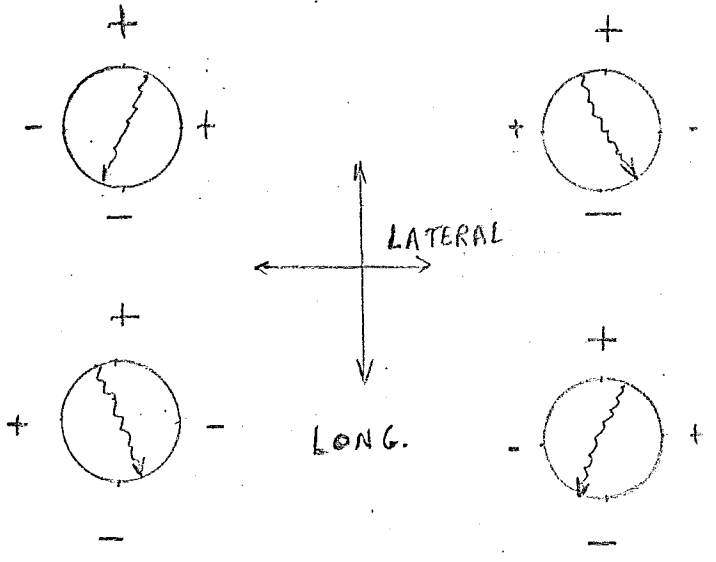

Fig. 38 Direction of Principal Stresses and Crack Growth on Tieplate Rivets

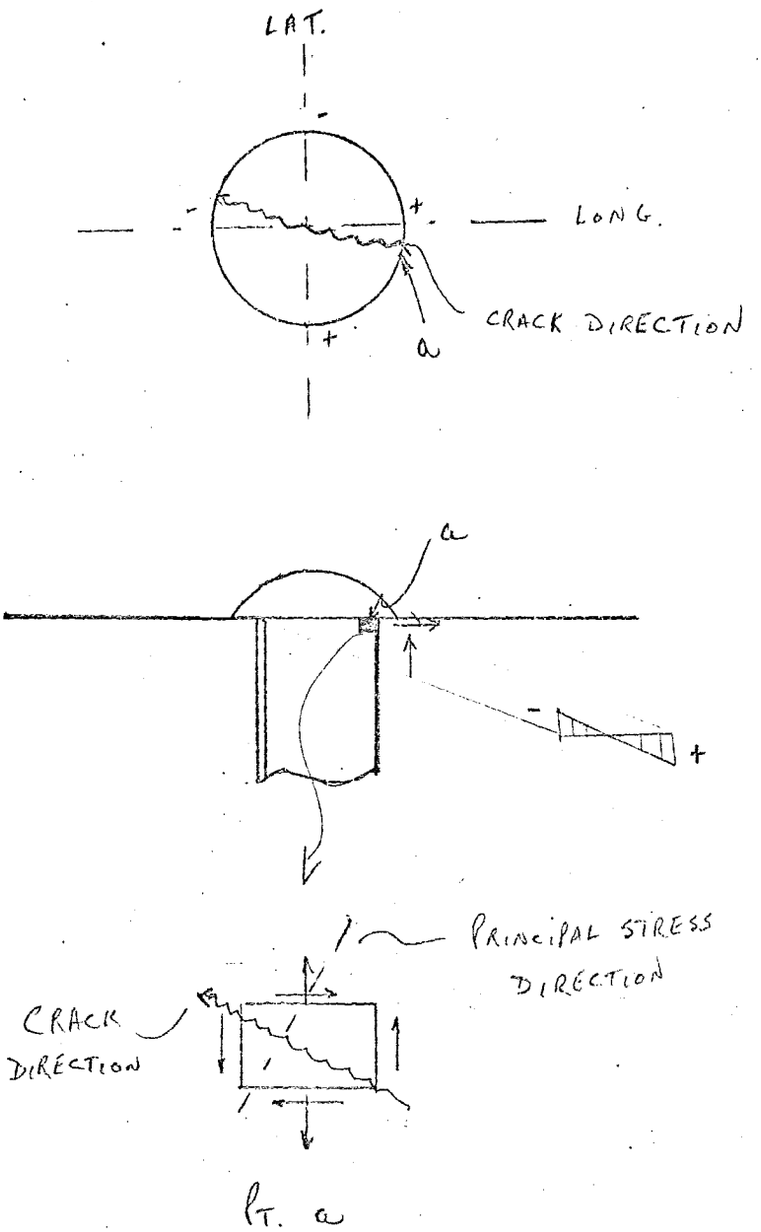

Fig. 39 Cause of Crack Growth into Head of Tieplate Rivet

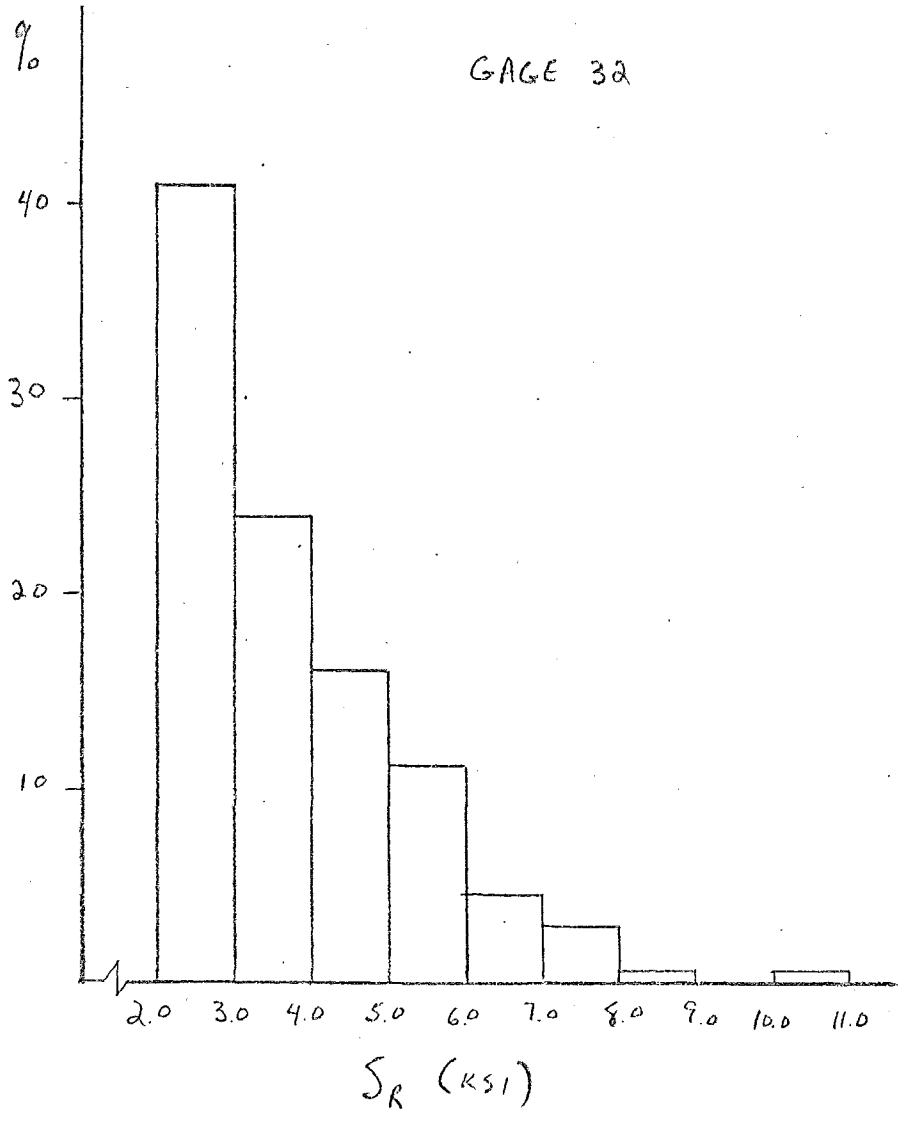

Fig. 40 Histogram for Gage 32 (South Bridge)

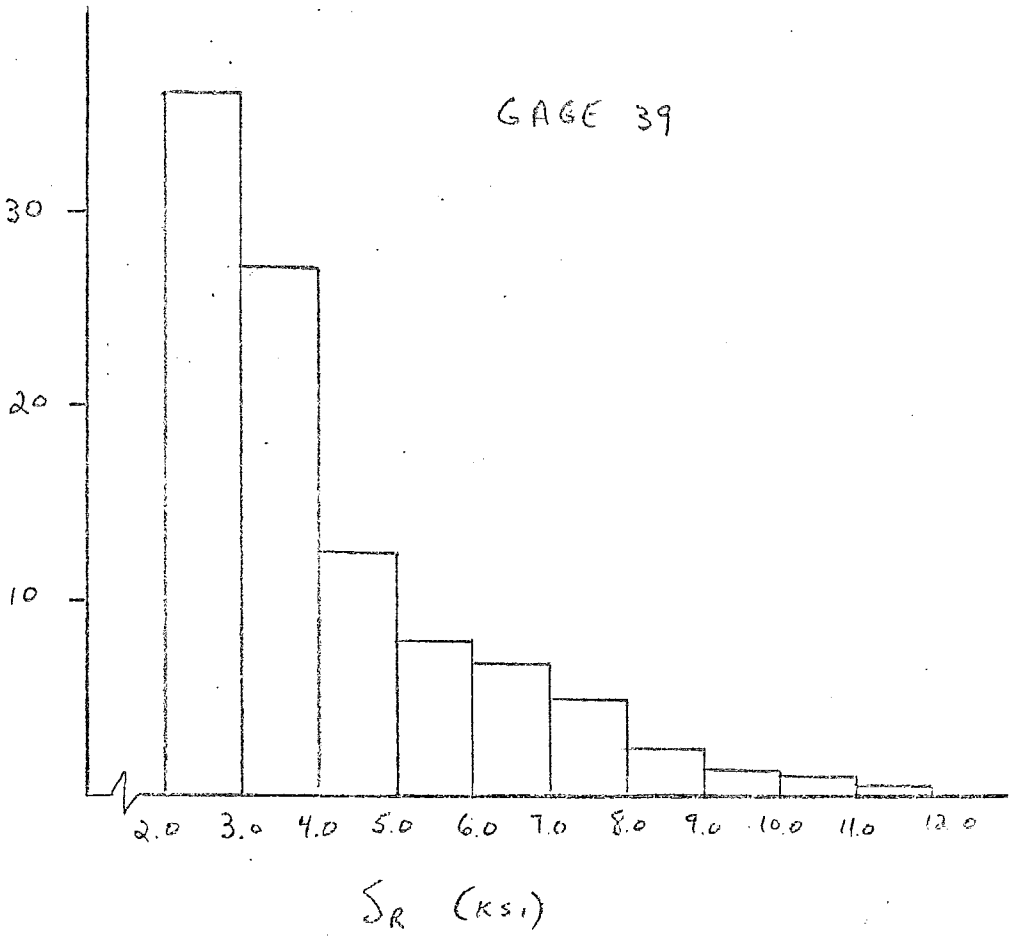

Fig. 41 Histogram for Gage 39 (South Bridge)

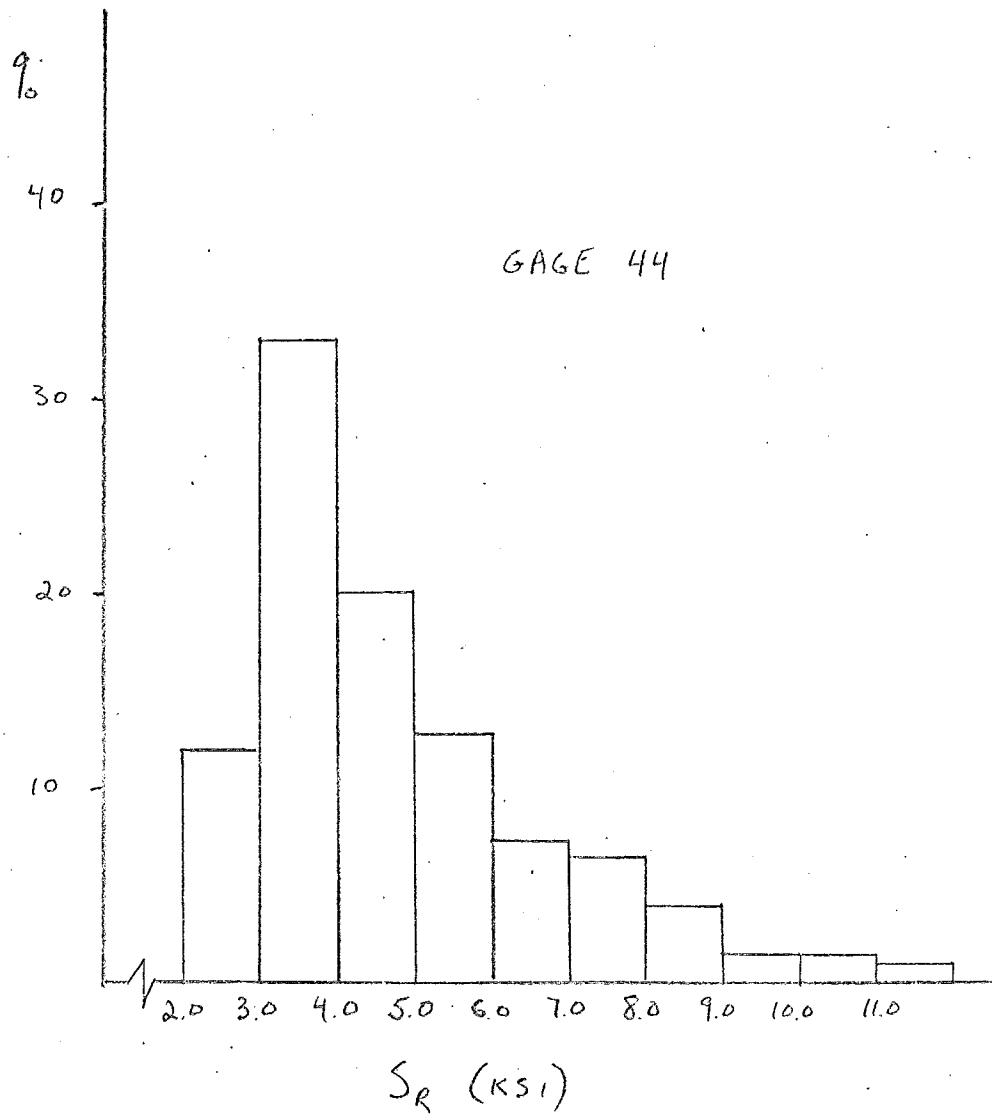

Fig. 42 Histogram for Gage 44 (South Bridge)

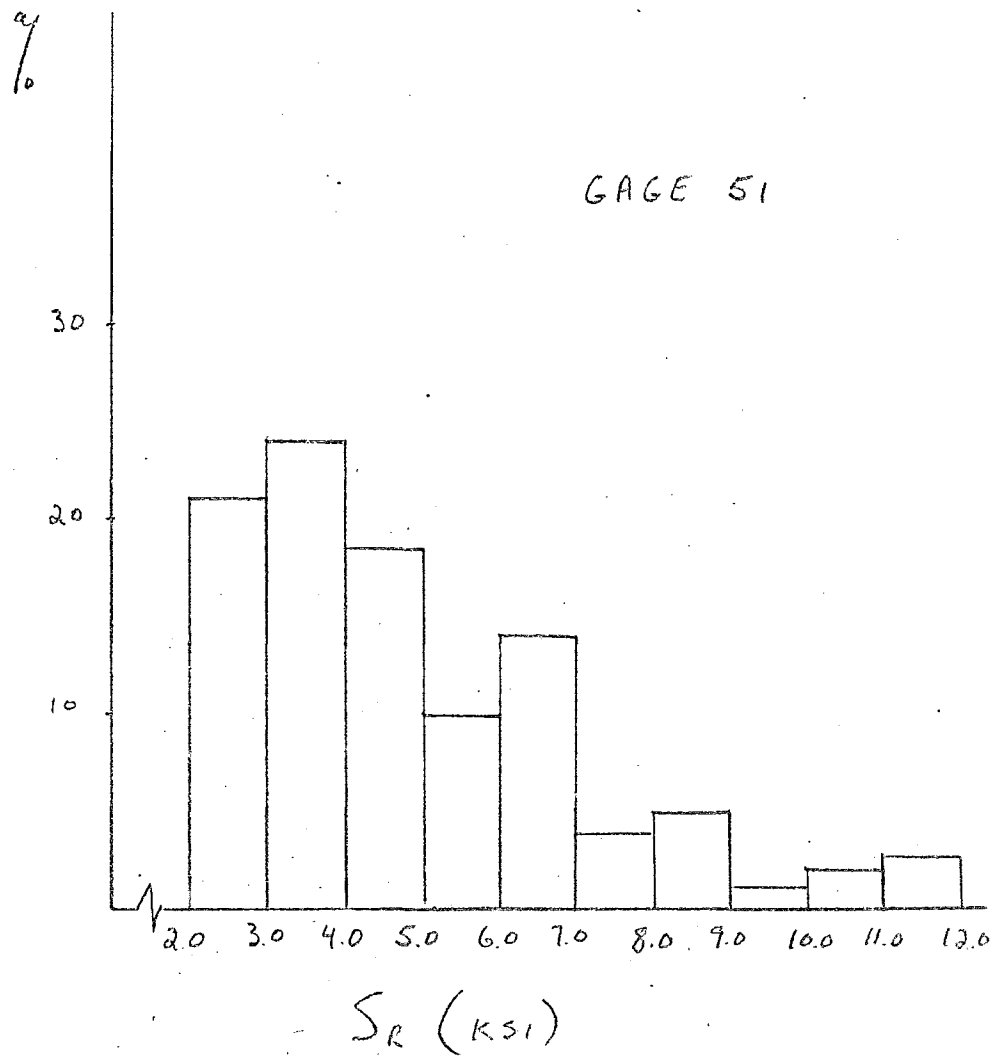

Fig. 43 Histogram for Gage 51 (South Bridge)

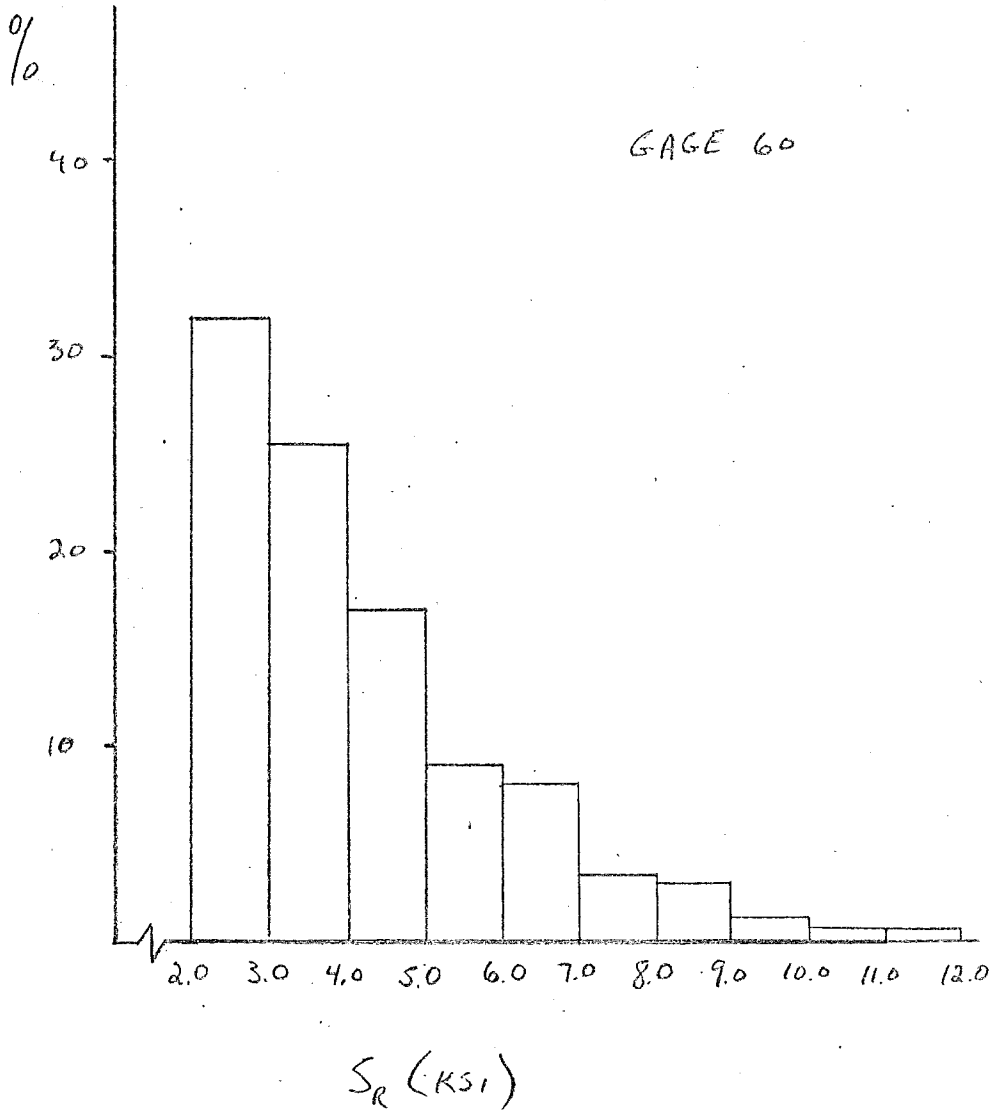

Fig. 44 Histogram for Gage 60 (South Bridge)

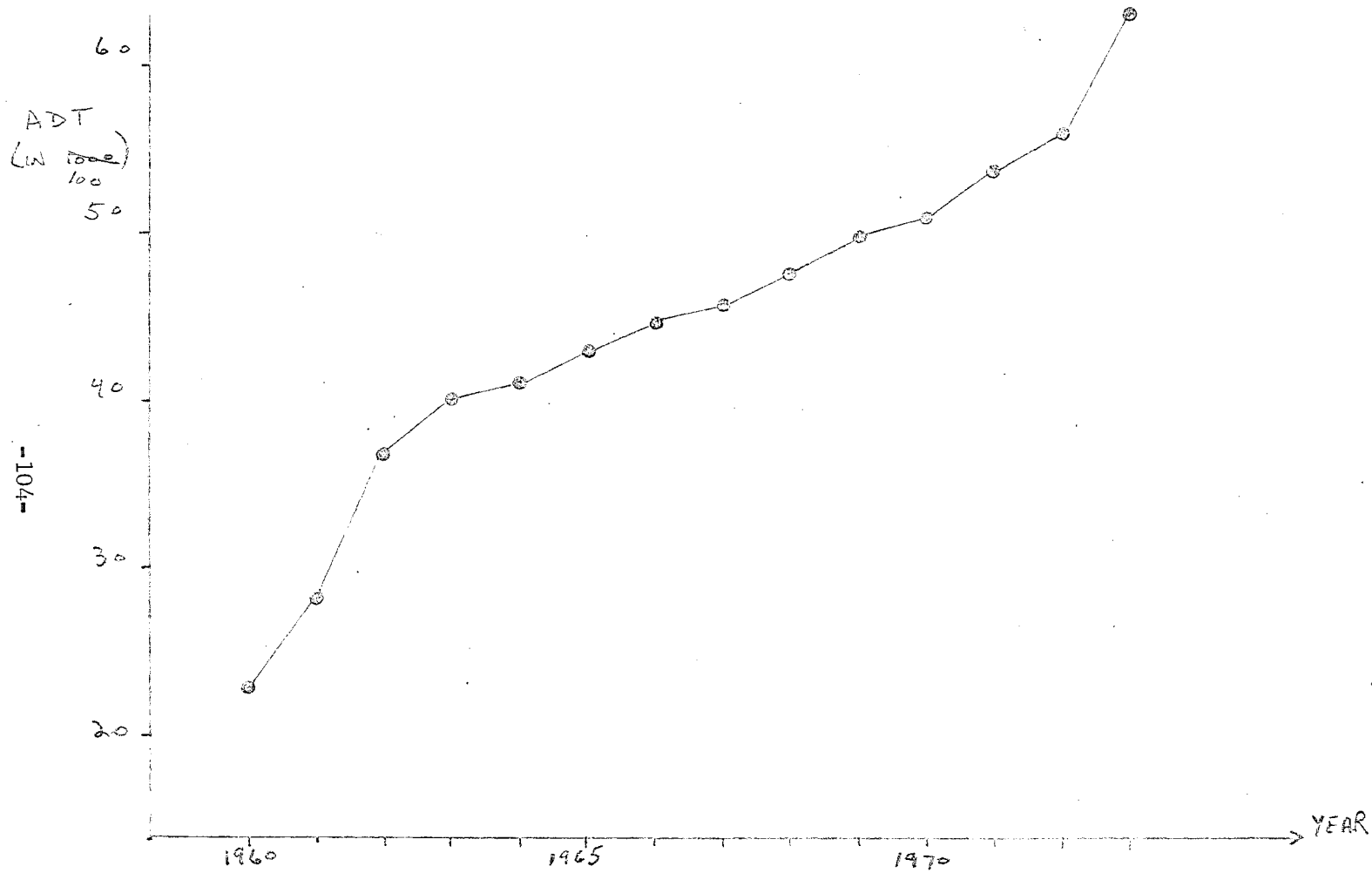

Fig. 45 Average Daily Traffic at South Bridge

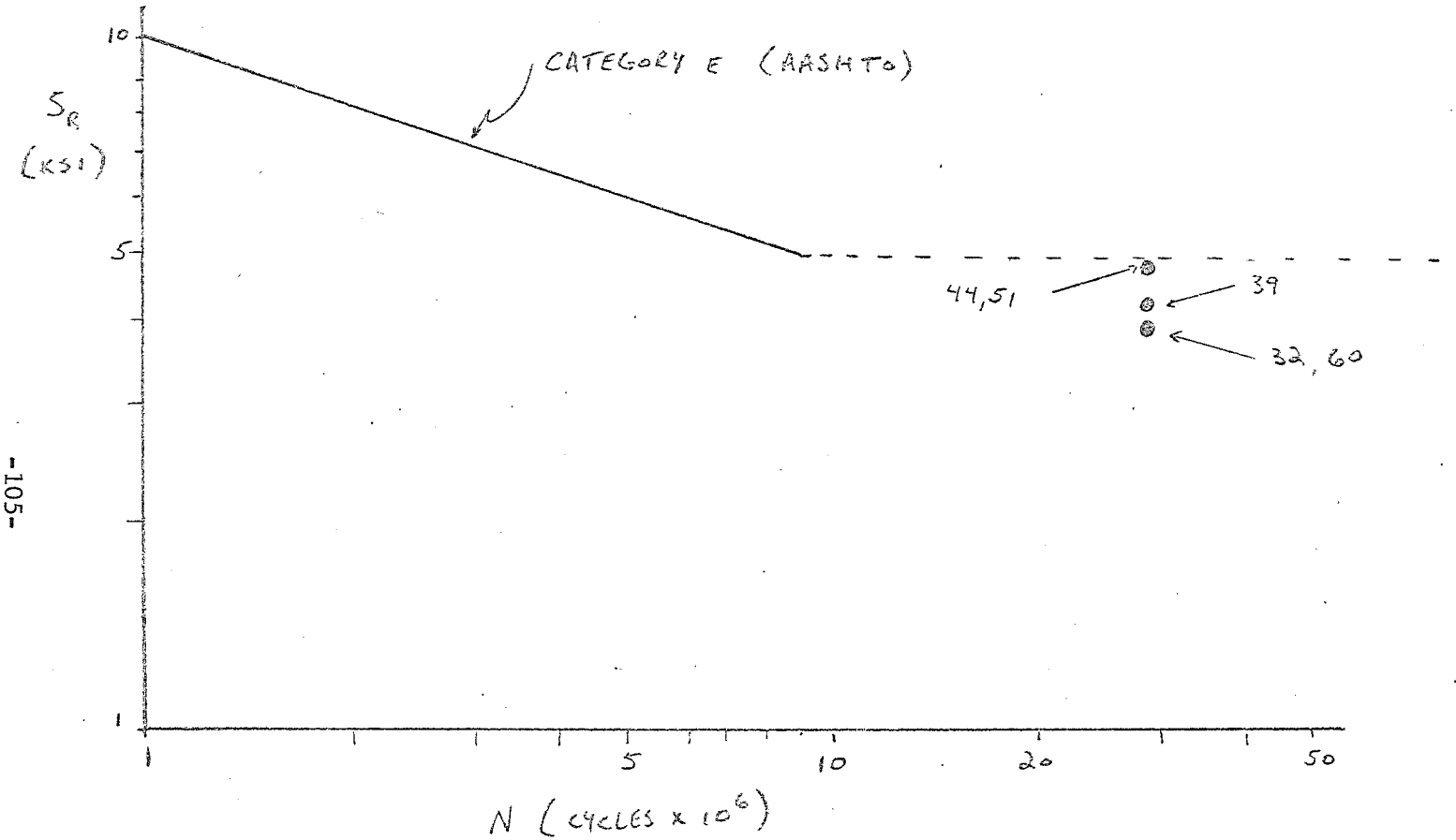

Fig. 46 Comparison of Root-Mean-Square Estimates with AASHTO Category E

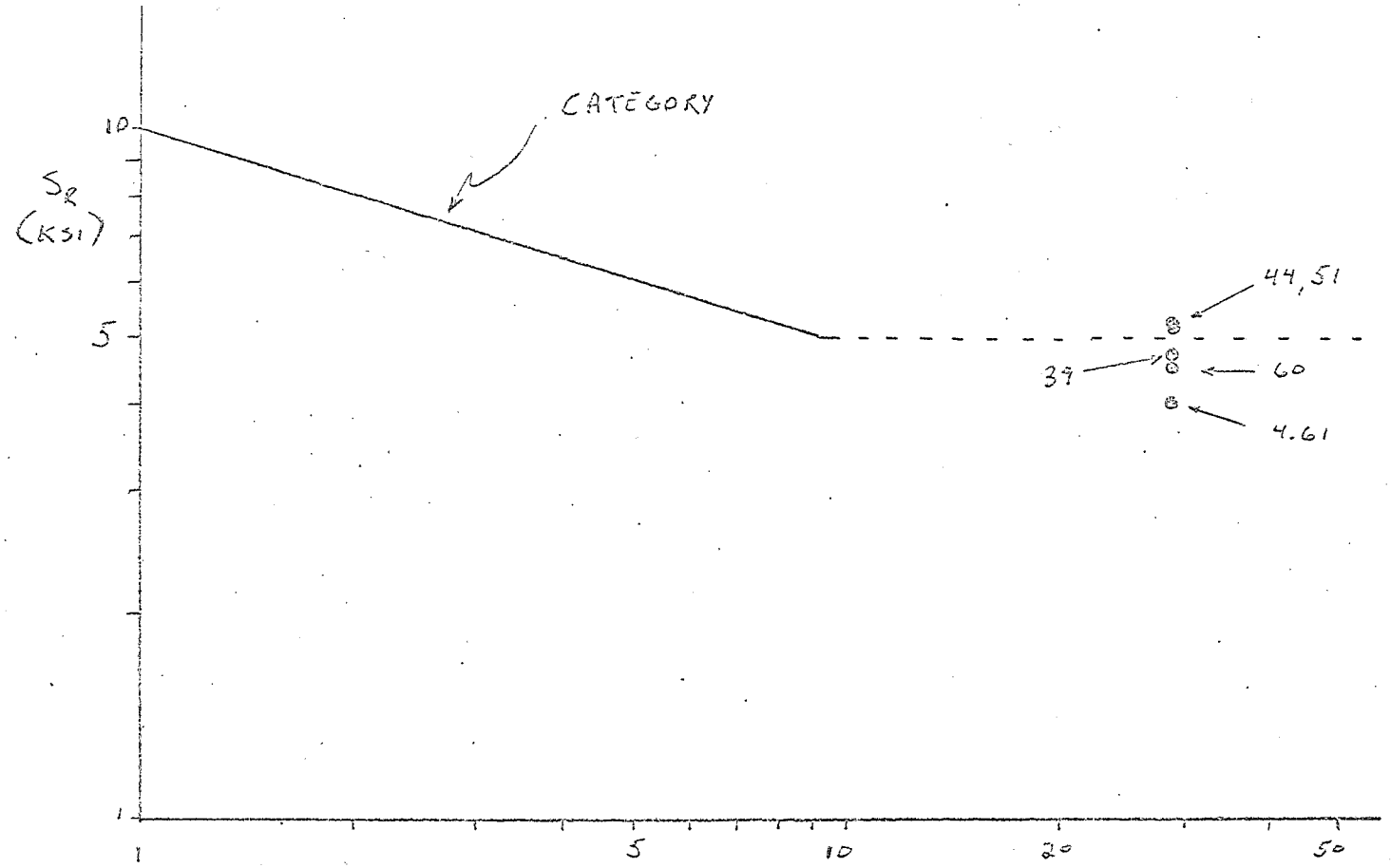

Fig. 47 Comparison of Miner's Hypothesis with AASHTO Category E

REFERENCES

1. Marchica, N. V., Yen, B. T. and Fisher, J. W.
   STRESS HISTORY STUDY OF THE ALLEGHENY BRIDGE (PENNSYLVANIA TURNPIKE), Fritz Engineering Laboratory Report No. 386.3, Lehigh University, May 1974.

2. Fisher, J. W., Yen, B. T. and Marchica, N. V.
   FATIGUE DAMAGE IN THE LEHIGH CANAL BRIDGE, Fritz Engineering Laboratory Report No. 386.1, Lehigh University, November 1974.

3. Bowers, D. G.
   LOADING HISTORY SPAN NO. 10, YELLOW MILL POND BRIDGE I-95, BRIDGEPORT, CONNECTICUT, Research Project HPR-175-332, Connecticut Department of Transportation, May 1972.

4. King, J. P. C., Csagoly, P. F. and Fisher, J. W.
   FIELD TESTING OF THE AQUASABON RIVER BRIDGE, ONTARIO, Prepared for presentation at the Transportation Research Board Annual Meeting, Washington, D. C., January 1985.

5. Fisher, J. W., Frank, K. H., Hirt, M. A. and McNamee, B. M.
   EFFECT OF WELDMENTS ON THE FATIGUE STRENGTH OF STEEL BEAMS, NCRHP Report No. 102, Highway Research Board, National Academy of Sciences-National Research Council, Washington, D. C., 1970.

6. Fisher, J. W., Albrecht, P. A., Yen, B. T., Klingerman, D. J. and McNamee, B. M.
   FATIGUE STRENGTH OF STEEL BEAMS WITH TRANSVERSE STIFFENERS AND ATTACHMENTS, NCHRP Report No. 147, Highway Research Board, National Academy of Sciences - National Research Council, Washington, D. C., 1974.

7. Pennsylvania Department of Transportation
   INSPECTION REPORT for L. R. 767, Cumberland and Dauphin Counties, Safety Update - John Harris Bridge, October 1974.

8. Galambos, C. F. and Armstrong, W. L.
   LOADING HISTORY OF HIGHWAY BRIDGES, U. S. Department of Transportation, Bureau of Public Roads, January 1969.

9. Cudney, G. R.
   THE EFFECTS OF LOADING ON BRIDGE LIFE, Highway Research Record No. 253, Highway Research Board, Division of Engineering, National Research Council, National Academy of Sciences - National Academy of Engineering, Washington, D. C., 1972.

REFERENCES (continued)

10. McKeel, W. T., Jr., Maddox, C. E., Jr., Kinnier, H. L. and Galambos, C. F.
LOADING HISTORY STUDY OF TWO HIGHWAY BRIDGES IN VIRGINIA, Highway Research Record No. 382, Highway Research Board, Division of Engineering, National Research Council, National Academy of Sciences - National Academy of Engineering, Washington, D. C., 1972.

11. Armstrong, W. L.
DYNAMIC TESTING OF CURVED BRIDGE - HUYCK STREAM, Journal of the Structural Division, Proceedings of ASCE, Col. 98, ST 9, September 1972.

12. Moses, F. and Carson, R.
PROBABILITY THEORY FOR HIGHWAY BRIDGE FATIGUE STRESSES, Final Report, Ohio Department of Transportation, SMSMD No. 50, Case Western Reserve University, Cleveland, Ohio, July 1973.

13. American Association of State Highway Transportation Officials Interim Specifications Bridges, 1974.

14. Fisher, J. W. and Struik, J.
GUIDE TO DESIGN CRITERIA FOR BOLTED AND RIVETED JOINTS, Wiley Interscience, 1974.

15. Fisher, J. W. and Daniels, J. H.
FIELD EVALUATION OF TIE PLATE GEOMETRY, Fritz Engineering Laboratory Report No. 386.4 (Draft), November 1974.

16. Schilling, C. G., Klippstein, K. H., Barsom, J. M. and Blake, G. T.
FATIGUE OF WELDED STEEL BRIDGE MEMBERS UNDER VARIABLE AMPLITUDE LOADING, Research Results Digest No. 60, Highway Research Board, 1974.

17. Swanson, S. R.
RAMDOM LOAD FATIGUE TESTING: A STATE OF THE ART SURVEY, ASTM, Materials Research and Standards, Vol. 8, No. 4, April 1968.

18. Barsom, J. M.
FATIGUE CRACK GROWTH UNDER VARIABLE AMPLITUDE LOADING IN ASTM A514-B STEEL, ASTM STP536, 1973.

19. Miner, M. A.
CUMULATIVE DAMAGE IN FATIGUE, Journal of the Applied Mechanics, Vol. 12, No. 1, September 1945.

APPENDIX A

LOCATION OF GAGES ON FIGS. 13-19

Columbia-Wrightsville Bridge

Gage	A (in.)	B (in.)	C (in.)	D (in.)	E (in.)	F (in.)	G (in.)	H (in.)	I (in.)
1				10-3/16	1				
2				6-3/4	1				
3				1	1				
4				9-7/16	1				
5				5-3/4	1				
6				15/16	1				
7	1-1/2	0							
8	6-1/2	0							
9	1-1/4	2							
10	6-3/4	2							
11	6-1/2	0							
12	1-1/2	0							
13						1	5		
14						1	5		
15								1	1
16	2	0							
17	6-1/2	0							
18	6-3/4	1-1/4							
19	1-1/2	1-1/2							
20	6-1/2	0							
21	2	0							
22						1	5		
23	6-1/2	0							
24	1-1/2	0							
27	6-1/2	1-1/2							
28	1	1							
29	1	1-1/2							
30	7	3/4							

APPENDIX A (continued)

LOCATION OF GAGES ON FIGS. 13-19

West Chester Bridge

Gage	D (in.)	L (in.)	M (in.)	N (in.)	O (in.)	P (in.)	Q (in.)
1	9-1/4						
2	5						
3	3/4						
4	9						
5	5						
6	1						
7	9						
8	5						
9	1						
10				3/4		1/4	
11		1-3/4	31-3/4				
12				3/4		3/16	
13				3/4		3/16	
14	9						
15	5						
16	1						
17	8-3/4						
18	5						
19	1-1/4						
20	9-1/4						
21	5						
22	3/4						
23							7-1/8
24				1		3/4	
25				1	3/4		
26				3/4		1/2	
27		1-3/4	44				
28							7-1/8
29				1		3/4	
30				1	3/4		

APPENDIX A (continued)

LOCATION OF GAGES ON FIGS. 13-19

South Bridge

Gage	A (in.)	B (in.)	C (in.)	J (in.)	K (in.)
11	1	1			
12	11-1/2	1			
13	24	1			
14	1		1		
15	12-1/2		1		
16	24		1		
17	1	1			
18	12-1/2	1			
19	24	1			
20	1		1		
21	11-1/2		1		
22	24		1		
23	22	1			
24	11-1/2	1			
25	1	1			
26	22		1		
27	11-1/2		1		
28	1		1		
29	24				
30	12-1/2				
31	1				
32	24				
33	12-1/2				
34	1				
35			19	6	
36				1	6
39	1	1			

APPENDIX A (continued)

LOCATION OF GAGES ON FIGS. 13-19

South Bridge (continued)

Gage	A (in.)	B (in.)	C (in.)	J (in.)	K (in.)
40	12-1/2	1			
41	24	1			
42	24		1		
43	12-1/2		1		
44	1		1		
46	15	1			
47	8	1			
48	1	1			
49	15		1		
50	8		1		
51	1		1		
52				19	8
53				1	8
54	1	1			
55	8	1			
56	15	1			
57	1		1		
58	8		1		
59	15		1		
60	1	1			
61	11-1/2	1			
62	22	1			
63	1		1		
64	11-1/2		1		
65	22		1		
66	22		1		
67	1		1		

APPENDIX A (continued)

LOCATION OF GAGES ON FIGS. 13-19

Interstate Route 81 Susquehanna River Bridge

Gage	F (in.)	G (in.)	H (in.)	I (in.)	R (in.)	S (in.)
1	2	6				
2	2	6				
4					2	
5						2
6			2	1		
7					2	
11	2	6				
12	2	6				
14	2	6				
15	2	6				
16			2	1		

VITA

Andrew C. Coates, the son of Cecelia and Eugene J. Coates, was born on January 3, 1952 in Brooklyn, New York. The author attended St. Anthony's High School in Smithtown, New York where he graduated with honors. He was a Dean's List student at Manhattan College where he recieved a Bachelor of Engineering Degree in Civil Engineering in May 1973. He was awarded a Research Assistantship in Civil Engineering at Fritz Engineering Laboratory, Lehigh University in September 1973 and received his Master of Science in Civil Engineering from Lehigh University in May, 1975.